The Plant Cell, Vol. 21: 3133–3151, October 2009, www.plantcell.org

NO VEIN Mediates Auxin-Dependent Specification and Patterning in the *Arabidopsis* Embryo, Shoot, and Root [W]

Ryuji Tsugeki,[a,1] Franck Anicet Ditengou,[b,c] Yoshinori Sumi,[a] William Teale,[b,c] Klaus Palme,[b,c,d] and Kiyotaka Okada[e]

[a] Department of Botany, Graduate School of Science, Kyoto University, Sakyo-ku, Kyoto 606-8502, Japan
[b] Institute of Biology II, Faculty of Biology, Albert-Ludwigs-Universität Freiburg, D-79104 Freiburg, Germany
[c] Centre for Biological Signaling Studies, Albert-Ludwigs-Universität Freiburg, D-79104 Freiburg, Germany
[d] Freiburg Institute of Advanced Sciences, Albert-Ludwigs-Universität Freiburg, D-79104 Freiburg, Germany
[e] Laboratory of Plant Organ Development, National Institute for Basic Biology, Myodaiji, Okazaki 444-8585, Japan

Local efflux-dependent auxin gradients and maxima mediate organ and tissue development in plants. Auxin efflux is regulated by dynamic expression and subcellular localization of the PIN auxin-efflux proteins, which appears to be established not only through a self-organizing auxin-mediated polarization mechanism, but also through other means, such as cell fate determination and auxin-independent mechanisms. Here, we show that the *Arabidopsis thaliana NO VEIN* (*NOV*) gene, encoding a novel, plant-specific nuclear factor, is required for leaf vascular development, cellular patterning and stem cell maintenance in the root meristem, as well as for cotyledon outgrowth and separation. *nov* mutations affect many aspects of auxin-dependent development without directly affecting auxin perception. *NOV* is required for provascular PIN1 expression and region-specific expression of PIN7 in leaf primordia, cell type–specific expression of PIN3, PIN4, and PIN7 in the root, and PIN2 polarity in the root cortex. *NOV* is specifically expressed in developing embryos, leaf primordia, and shoot and root apical meristems. Our data suggest that *NOV* function underlies cell fate decisions associated with auxin gradients and maxima, thus establishing cell type–specific PIN expression and polarity. We propose that *NOV* mediates the acquisition of competence to undergo auxin-dependent coordinated cell specification and patterning, thereby eliciting context-dependent auxin-mediated developmental responses.

INTRODUCTION

In plants, the phytohormone auxin has been established as a key regulator of axial patterning processes. Local auxin gradients associated with auxin maxima mediate pattern formation in the root (Sabatini et al., 1999; Friml et al., 2002a; Blilou et al., 2005), lateral organ (Reinhardt et al., 2000, 2003; Benková et al., 2003), embryo (Liu et al., 1993; Steinmann et al., 1999; Friml et al., 2003), and vascular tissue (Sachs, 1991; Mattsson et al., 1999; Sieburth, 1999; Mattsson et al., 2003). By contrast, organ separation is associated with local reductions in auxin concentration (Heisler et al., 2005). Local auxin gradients direct formation of plant organs, regardless of their morphology or developmental origin (Benková et al., 2003). Cell type–specific expression and asymmetric subcellular localization of the PIN family of auxin-efflux proteins define auxin distribution, a central factor in the formation of auxin concentration gradients and maxima (Petrásek et al., 2006; Wisniewska et al., 2006). It has been shown that PIN expression and polarity are established not only through a self-organizing auxin-mediated feedback regulatory loop (Sieberer et al., 2000; Paciorek et al., 2005; Vieten et al., 2005; Sauer et al., 2006) but also through cell fate determination (Sauer et al., 2006; Xu et al., 2006), reversible phosphorylation of PIN proteins (Michniewicz et al., 2007), endocytic recycling (Geldner et al., 2001; Jaillais et al., 2007; Dhonukshe et al., 2008; Kleine-Vehn et al., 2008a), vesicle trafficking to vacuoles (Kleine-Vehn et al., 2008b; Shirakawa et al., 2009), protein turnover (Abas et al., 2006; Kleine-Vehn et al., 2008b; Spitzer et al., 2009), and auxin-independent mechanisms (Willemsen et al., 2003; Bennett et al., 2006). Physical stimuli also modulate PIN expression and polar localization, thus affecting plant architecture through triggering changes in efflux-dependent auxin distribution (Friml et al., 2002b; Ditengou et al., 2008; Laskowski et al., 2008; Laxmi et al., 2008). Feedback regulation between auxin signaling and transport constitutes a self-organizing auxin-mediated polarization and patterning mechanism. This mechanism links individual cell polarity with tissue and organ polarity (Sauer et al., 2006; Scarpella et al., 2006; Wenzel et al., 2007).

In roots, auxin transport and the auxin response are essential for correct expression of the cell fate regulators *PLETHORA* (*PLT*) and *SCARECROW* (*SCR*) (Friml et al., 2002a; Sabatini et al., 2003; Aida et al., 2004; Blilou et al., 2005), suggesting that auxin and auxin flow regulate cell fate. Reciprocally, the cell fate regulators appear to control the polarity of auxin flow in roots (Blilou et al., 2005; Xu et al., 2006). Therefore, in roots, cell fate determinants appear to be integrated into the positive feedback loop that controls the polarization of auxin flow and polarized organ development.

[1] Address correspondence to rtsugeki@ok-lab.bot.kyoto-u.ac.jp.
The author responsible for distribution of materials integral to the findings presented in this article in accordance with the policy described in the Instructions for Authors (www.plantcell.org) is: Ryuji Tsugeki (rtsugeki@ok-lab.bot.kyoto-u.ac.jp).
[W] Online version contains Web-only data.
www.plantcell.org/cgi/doi/10.1105/tpc.109.068841

In shoots, auxin maxima mark sites of incipient primordia (Heisler et al., 2005) and leaf venation (Mattsson et al., 2003; Scarpella et al., 2006). Externally applied auxin initiates primordium outgrowth (Reinhardt et al., 2000) and vascular formation (Sachs, 1991; Sauer et al., 2006) de novo. The earliest sign of vascular differentiation in leaves is the expression of PIN1 in presumptive preprocambial cells (Scarpella et al., 2006; Bayer et al., 2009), which arises among seemingly equivalent subepidermal cells. Hereafter, we collectively refer to preprocambial and procambial cells as provascular cells. PIN1 directs auxin flow to converge in the marginal epidermis of developing leaf primordia. Concomitantly, this creates adjacent subepidermal auxin maxima, which give rise to the distal ends of presumptive provascular strands (Scarpella et al., 2006). Thus, it was proposed that the epidermal convergence points of auxin flow externally determine the sites of provascular formation and trigger auxin-mediated provascular patterning in the ground meristem. However, the molecular mechanism that establishes the provascular expression and polarity of PIN proteins remains largely unknown. Other important open questions are the mechanisms by which (1) auxin maxima are generated in internal tissues and (2) how auxin maxima induce cell specification and patterning.

Here, we describe the *NO VEIN* (*NOV*) gene of *Arabidopsis thaliana*. It encodes a novel plant-specific nuclear factor required for leaf vascular development, cellular patterning and stem cell maintenance in the root meristem, as well as for cotyledon outgrowth and separation. Embryonic apical-basal patterning, vascular continuity, and shoot-derived organ separation become defective when polar auxin transport is additionally impaired in *nov-1*, either chemically or genetically, further supporting the important role of *NOV* in auxin-mediated development. *nov* mutations affect many aspects of auxin-dependent development without directly affecting auxin perception. *NOV* is required for the cell type–specific expression and polarity of PIN proteins during leaf primordium and root development. *NOV* is specifically expressed in developing embryos, leaf primordia, lateral root primordia, and the meristematic region of shoots and roots. Our data suggest that *NOV* function underlies cell fate decisions associated with auxin gradients and maxima, thus establishing PIN expression and polarity in a cell type–specific manner. We propose that *NOV* is involved in endowing cells with the competence to undergo auxin-dependent coordinated cell specification and patterning, thereby eliciting context-dependent auxin-mediated developmental responses during formation of plant organs and tissues, regardless of their morphology and developmental origin.

RESULTS

NOV Is Required for Vascular Formation in Leaves

To understand the mechanisms of leaf provascular development, we isolated *Arabidopsis* mutants defective in leaf vein formation (see Methods). *nov-1* was identified as a recessive mutant showing narrow rosette leaves with far fewer veins than those of the wild type (cf. Figures 1B and 1C with 1A). Occasionally, *nov-1* plants never formed veins in their first two rosette leaves (Figure 1C). Four T-DNA insertion alleles with stronger phenotypes, *nov-2*, *-3*, *-4*, and *-5*, were also identified (Figure 8A). Hereafter, all four T-DNA alleles are collectively described as *nov-2*~*5*. While *nov-2*~*5* usually exhibit an embryo-defective phenotype (Figure 3), *nov-3* seedlings were infrequently detected among the progeny of heterozygous *nov-3* plants. In *nov-3* seedlings, no leaf vein was observed either in the first two rosette leaves, in the cotyledons (cf. Figure 1E with 1D), or in the adult-phase rosette leaves (cf. Figure 1G with 1F). These results suggest that *NOV* is required for vascular formation in cotyledons and leaves. In *nov-1* leaf primordia, the expression of the pre-pro/procambium markers *ARABIDOPSIS THALIANA HOMEOBOX 8* (*ATHB8*) and *J1511-green fluorescent protein* (*GFP*) was either downregulated or undetectable (cf. Figures 1J with 1H and 1I; cf. Figures 1L and 1N with 1K and 1M, respectively; cf. Supplemental Figure 1B with 1A online), suggesting that *NOV* is necessary for the formation of provascular cells in leaves.

In wild-type plants, during leaf development, auxin/indole-3-acetic acid-auxin response factor-dependent transcription from the *DR5* promoter is detected in provascular cells (Ulmasov et al., 1997; Mattsson et al., 2003; Figure 1O). In *nov-1*, *DR5* expression in leaves was disrupted (cf. Figure 1P with 1O; cf. Figures 1T and 1V with 1S and 1U, respectively) and often confined to the epidermis of the leaf margin (Figures 1P and 1V). However, the ability to respond to exogenous auxin in *nov-1* was comparable to that in the wild type (cf. Figure 1R with 1Q), indicating that *NOV* is not necessary for auxin/indole-3-acetic acid-auxin response factor–dependent gene expression. These data suggest that *NOV* is required for proper auxin distribution during leaf development.

NOV Is Required for Root Development

Roots of *nov-1* were shorter than those of the wild type (cf. Figure 2B with 2A), implying that *NOV* also functions in root development. Compared with the wild type (Figures 2G and 2I), cellular organization of the root meristem was disarranged in *nov-1* (Figures 2H and 2J) and *nov-3* (Figure 2K). An auxin maximum, which establishes a distal organizer in the root (Sabatini et al., 1999), was detected at the quiescent center in *nov-1* (Figure 2J) and *nov-3* (Figure 2K) mutants, as in the wild type (Figures 2I). These results suggest that *NOV* is required for auxin-mediated cellular patterning in the root tip.

Mature columella root cap cells contain starch granules that are not seen in their stem cells (van den Berg et al., 1997; Figure 2C; see Supplemental Figure 2A online). In *nov-1* (Figure 2D) and *nov-3* (see Supplemental Figure 2B online), starch granules were also detected in columella stem cells, suggesting that *NOV* is required for columella stem cell maintenance. The maintenance of cortex/endodermis stem cells requires two successive cell divisions with the cortex/endodermis stem cell first undergoing an anticlinal cell division. The basal daughter cell is then maintained as a stem cell, and the apical cell divides periclinally, giving rise to cortex and endodermis cells. In *nov-1* (Figure 2J, asterisks) and *nov-3* (see Supplemental Figure 3B online), the cortex/endodermis stem cells underwent a periclinal division without a prior anticlinal division (cf. Figures 2G and 2I; see Supplemental Figure 3A online; see also Figures 3E to 3G). Therefore, *NOV* is required to maintain root stem cells for the cortex and endodermis. We observed ectopic divisions in the

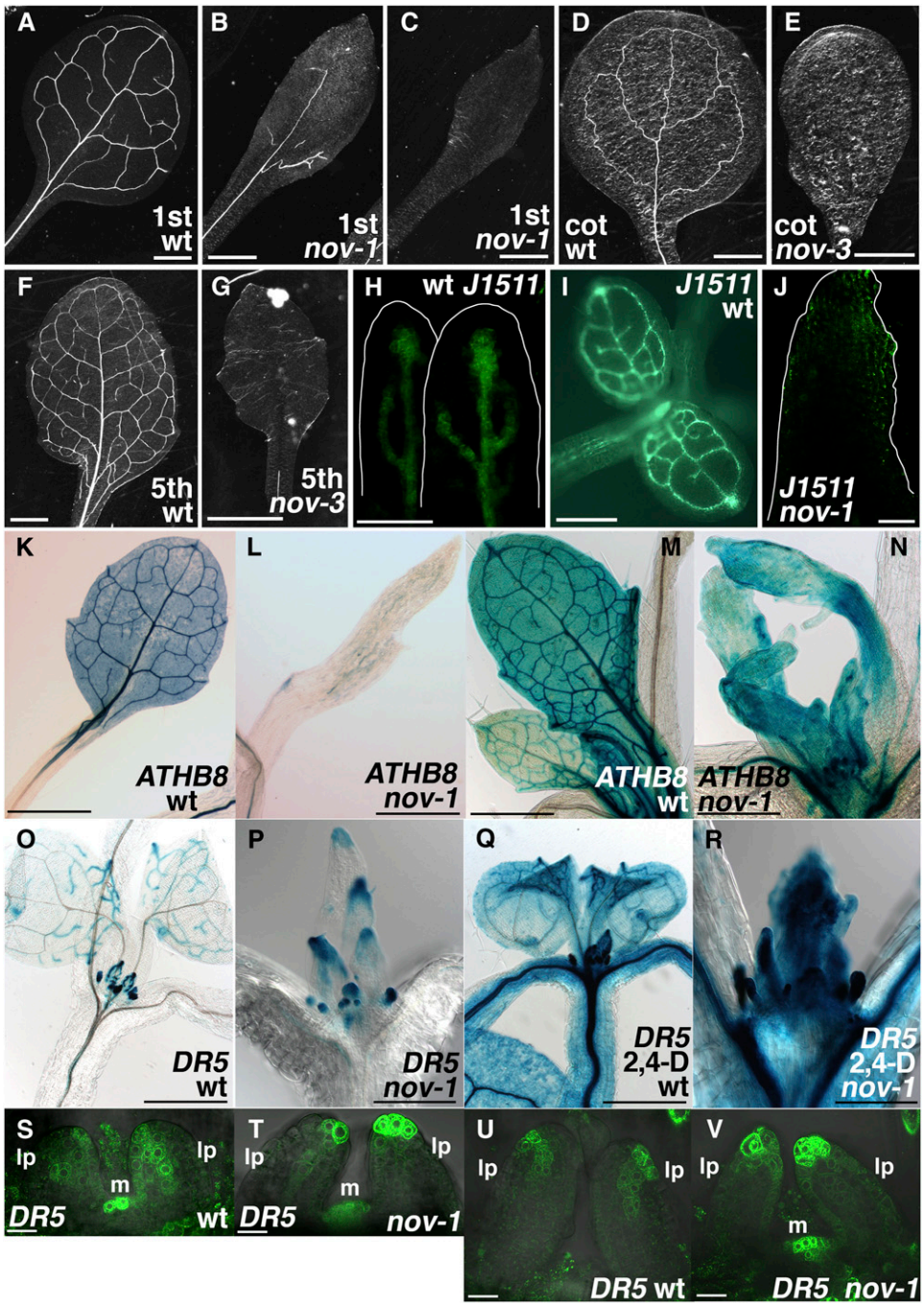

Figure 1. Leaf Phenotype in *nov* Mutants.

(A) to **(G)** Leaf venation pattern. Cleared samples of the first or second rosette leaves of 19-d-old wild type (C24 in **[A]**) and *nov-1* (**[B]** and **[C]**). Cotyledons and fifth rosette leaves of 38-d-old wild type (Col in **[D]** and **[F]**) and *nov-3* (**[E]** and **[G]**), respectively.

(H) to **(N)** Expression of provascular markers. Wild-type leaf primordia show *J1511-GFP* (**[H]** and **[I]**) and $ATHB8_{pro}$*:GUS* (**[K]** and **[M]**) expression in provascular cells. *nov-1* develops leaf primordia with no *J1511-GFP* **(J)** or $ATHB8_{pro}$*:GUS* expression in provascular cells (**[L]** and **[N]**).

(O) to **(V)** Expression of the auxin response marker *DR5* in wild type ($DR5_{pro}$*:GUS* in **[O]** and **[Q]**; $DR5_{pro}$*:GFP* in **[S]** and **[U]**) and *nov-1* ($DR5_{pro}$*:GUS* in **[P]** and **[R]**; $DR5_{pro}$*:GFP* in **[T]** and **[V]**). In the presence of the synthetic auxin, 2,4-D, *DR5* is similarly expressed in wild type **(Q)** and *nov-1* **(R)**. Samples in **(K)** to **(T)** are taken from plants grown at 27°C, as *nov-1* phenotype is strengthened at higher temperature. For comparison, *ATHB8* expression at 27°C (**[L]** and **[N]**) and at 21 to 22°C (see Supplemental Figure 1 online) is shown. lp, leaf primordium; m, shoot apical meristem.

Bars = 1 mm in **(A)** to **(G)**, **(K),** and **(L)**, 50 μm in **(H)** and **(J)**, 0.5 mm in **(I)**, **(M)** to **(O)**, and **(Q)**, 0.25 mm in **(P)** and **(R)**, and 20 μm in **(S)** to **(V)**.

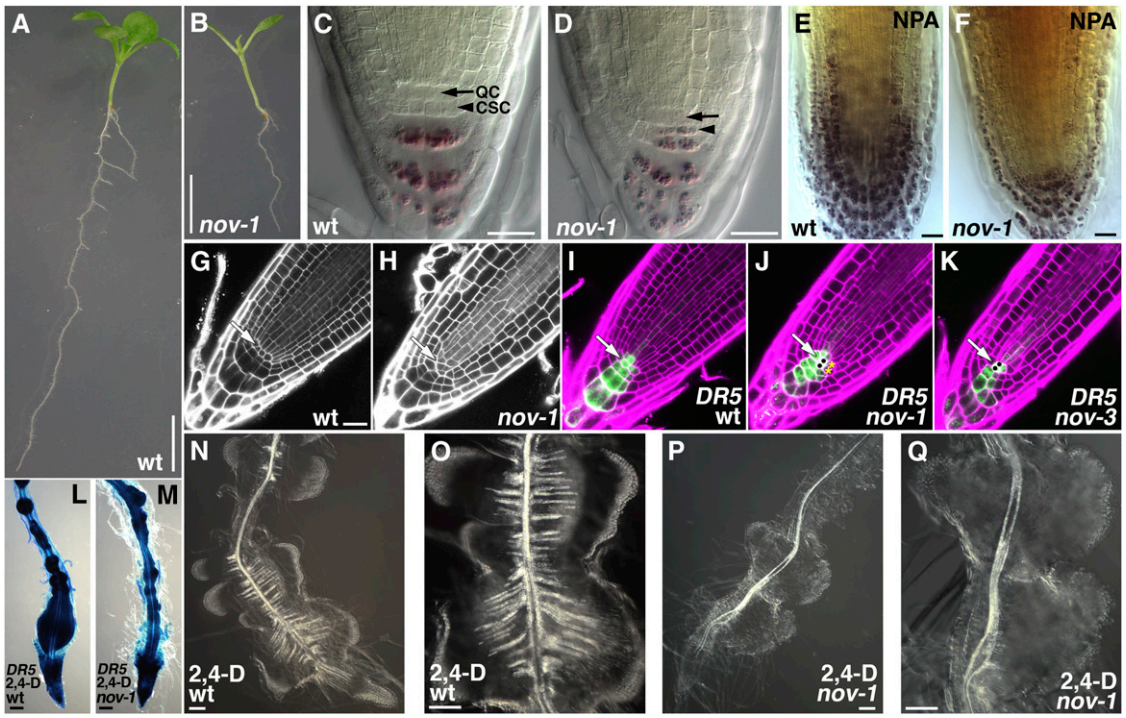

Figure 2. Root Phenotype in *nov* Mutants.

(A) and **(B)** Seedlings of wild type **(A)** and *nov-1* **(B)** grown for 12 d.
(C) and **(D)** Starch staining of root tips of the wild type **(C)** and *nov-1* **(D)**. Arrows and arrowheads indicate positions of the quiescent center (QC) and columella stem cells (CSC), respectively.
(E) and **(F)** Effect of NPA on root tips of the wild type **(E)** and *nov-1* **(F)**. Root tips were stained for starch.
(G) and **(H)** Propidium iodide staining of root tips of the wild type **(G)** and *nov-1* **(H)**.
(I) to **(K)** $DR5_{pro}$*:GFP* expression in root tips of the wild type **(I)**, *nov-1* **(J)**, and *nov-3* **(K)**. Cells resulting from an ectopic division in the quiescent center and cortex/endodermis stem cell are marked by black dots in **(J)** and **(K)** and by asterisks in **(J)**, respectively. White arrows in **(G)** to **(K)** indicate positions of the quiescent center
(L) to **(Q)** Effect of the synthetic auxin 2,4-D on roots of the wild type (**[L]**, **[N]**, and **[O]**) and *nov-1* (**[M]**, **[P]**, and **[Q]**). $DR5_{pro}$*:GUS* expression in roots of the wild type **(L)** and *nov-1* **(M)** treated with 2,4-D.
Bars = 5 mm in **(A)** and **(B)**, 20 μm in **(C)** to **(G)** (equal scale in **[G]** to **[K]**), and 100 μm in **(L)** to **(Q)**.

quiescent center in *nov-1* and *nov-3* (Figures 2J and 2K, black dots), presumably replacing the stem cells that failed to be maintained (see Supplemental Figure 5 online).

In wild-type plants, exogenous application of the synthetic auxin 2,4-D induced the formation of lateral root primordia, most of which were fused. These primordia had more xylem strands than the primary root (Figures 2N and 2O). Although 2,4-D also induced the formation of lateral root primordia in *nov-1*, xylem strand formation was either absent or greatly repressed in 2,4-D–induced lateral roots (Figures 2P and 2Q). There was no significant difference in auxin response (as detected by *DR5* expression) between wild-type and *nov-1* plants (Figures 2L and 2M). These results suggest that *NOV* is required for auxin-mediated vascular formation not only in leaves but also in roots.

NOV Is Required for Embryonic Development

NOV is required for auxin-mediated development in the leaf (Figure 1) and root (Figure 2), suggesting that *NOV* has a common function in auxin-mediated developmental processes. Consistent with this idea, the stronger T-DNA insertion alleles, *nov-2*~*5* (described below; Figure 8A), exhibited an embryo-defective phenotype characterized by size reduction and frequent fusion of cotyledons (Figures 3F to 3H and 3K to 3M; cf. developing wild-type embryos in Figures 3A to 3D, 3I, 3J, 3N, 3P, and 3R) and abnormalities in the early steps of vascular development (see Supplemental Figure 4 online). A similar phenotype has been observed in mutants either defective in polar auxin transport (Steinmann et al., 1999; Friml et al., 2003; Vieten et al., 2005) or auxin signaling (Hardtke et al., 2004).

The expression pattern of the pre-pro/procambium marker *J1511-GFP* in *nov-5* embryos further indicated fusion of cotyledons (cf. Figure 3H with 3D, early-heart to mid-heart stage embryos) and defective provascular development (cf. Figures 3K to 3M with 3I and 3J, mid-heart to late-heart stage and mature embryos). In *nov-5* embryos in which the cotyledons did not grow, expression of *J1511-GFP* seen in the apical part of wild-type embryos (Figures 3D, 3I, and 3J) was missing or greatly

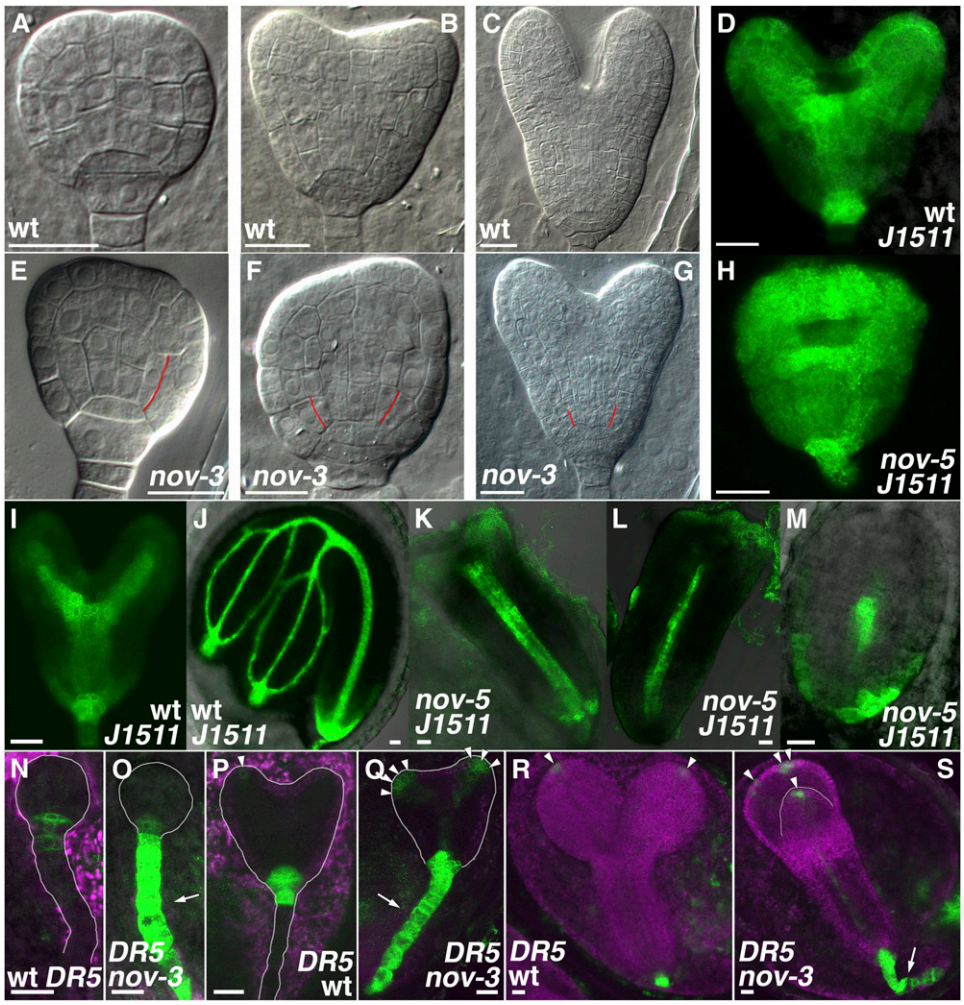

Figure 3. Embryonic Phenotype in *nov* Mutants.

(A) to **(M)** Embryos of the wild type (**[A]** to **[D]**, **[I]**, and **[J]**), *nov-3* (**[E]** to **[G]**), and *nov-5* (**[H]** and **[K]** to **[M]**). Wild-type embryos at the mid globular **(A)**, triangular to early-heart **(B)**, early-heart to mid-heart **(D)**, mid-heart to late-heart **(I)**, early-torpedo **(C)**, and mature-embryo **(J)** stages are shown as controls. Embryos of *nov-3* and *nov-5* are defective in cotyledon growth (**[F]** to **[H]** and **[K]** to **[M]**) and separation (**[G]**, **[H]**, and **[L]**) and maintenance of stem cells for cortex/endodermal cells (**[E]** to **[G]**; cell boundaries presumably caused by precocious periclinal division of cortex/endodermal cells are indicated by red lines). Embryos in **(D)** and **(H)** to **(M)** harbor *J1511-GFP*. In *nov-5*, provascular expression of *J1511-GFP* in cotyledon primordia is repressed or missing (**[K]** to **[M]**).

(N) to **(S)** $DR5_{pro}$*:GFP* expression in embryos of the wild type (**[N]**, **[P]**, and **[R]**) and *nov-3* (**[O]**, **[Q]**, and **[S]**). In embryos of *nov-3*, ectopic expression of *DR5* was detected in the suspensor (arrows in **[O]**, **[Q]**, and **[S]**) and tips of cotyledon primordia. *DR5* expression in tips of cotyledon primordia is marked by arrowheads in **(P)** to **(S)**.

Bars = 20 μm.

repressed (Figure 3M), suggesting that *NOV* is required for *J1511-GFP* expression in the apical part of embryos, which may correlate with development of cotyledon primordia. On the other hand, *nov-5* embryos showing some outgrowth of cotyledons exhibited *J1511-GFP* expression in the apical part, although provascular *J1511-GFP* expression tended to be missing or greatly repressed (Figures 3K and 3L). These results suggest that *NOV* is required for provascular formation in the apical part of embryos, which may promote development of cotyledon primordia. In wild-type embryos, from around the triangular stage, *DR5* expression is found mainly in the tips of cotyledon primordia and the uppermost cell of the suspensor (Benková et al., 2003; Friml et al., 2003; Figures 3N, 3P, and 3R). In *nov-3*, however, the area of *DR5* expression was expanded in the tips of cotyledon primordia and encompassed the entire suspensor (Figures 3O, 3Q, and 3S), suggesting that *NOV* is also required for proper auxin distribution in embryonic development.

In *nov-2*~*5* embryos, cortex/endodermis stem cells often underwent periclinal division without a prior anticlinal division and were lost (cf. Figures 3E to 3G with 3A to 3C; cf.

Supplemental Figure 5C with 5A online). As was observed in roots, an ectopic division was observed in the quiescent center (cf. Supplemental Figures 5C and 5D with 5A and 5B online). Judging from the expression of *SCR* and *SHORT ROOT* (*SHR*) (see Supplemental Figure 6 online), radial patterning appears to be normal in *nov-3* embryos.

Genetic Interaction of *NOV* and *GNOM*

GNOM is required for the proper subcellular localization of PIN proteins and therefore for polar auxin transport (Steinmann et al., 1999; Geldner et al., 2003; Kleine-Vehn et al., 2008a). To study the role of *NOV* in polar auxin transport-dependent organ development, the genetic interaction between *NOV* and *GNOM* was assessed. *gnom*^{R5} is a weak allele, invariably producing primary roots and displaying partial or complete fusion of cotyledons in about one-third of seedlings (Geldner et al., 2004; Figures 4A, 4P, and 4V). *nov-1 gnom*^{R5} occasionally lacked the root (Figures 4B to 4F, 4H, 4I, 4L, 4M, and 4R) and/or cotyledon (Figures 4D to 4F, 4R, and 4S) and resembled strong *gnom* alleles defective in apical-basal polarity (Mayer et al., 1993; Figure 4G). For comparison, plants of the wild type (Figures 4N and 4T) and *nov-1* (Figures 4O and 4U) are shown. Also segregated among *nov-1 gnom*^{R5} plants were seedlings with four to six cotyledons that were, to a greater or lesser extent, fused to each other (Figures 4H to 4M and 4Q). This phenotype was not seen in *nov-1*, *-2*, *-3*, *-4*, or *-5*, and neither has it been reported in *gnom* alleles, suggesting that *NOV* and *GNOM* are required redundantly for the determination of cotyledon number. A similar phenotype was observed in the double mutant of *nov-1* with another weak allele, *gnom*$^{B/E}$ (Geldner et al., 2004) (see Supplemental Figure 7 online). Defects in xylem strand continuity in *gnom*^{R5} (Geldner et al., 2004; Figure 4V) were enhanced in *nov-1 gnom*^{R5} (Figures 4C, 4I, 4M, and 4W). Here, in seedlings that produced roots, not only was xylem strand continuity repressed in the cotyledon, but also xylem differentiation was repressed at the cotyledon-hypocotyl junction (Figure 4W, arrow), where the protoxylem first differentiates (Pyo et al., 2004; cf. Figures 4T to 4V). All phenotypes described indicate that *NOV* is genetically redundant to *GNOM* in organ and tissue development associated with polar auxin transport.

The Effect of Inhibition of Polar Auxin Transport on the *nov-1* Mutant

Further analysis of the roles of *NOV* in auxin-mediated development focused on the effect of 1-naphthylphthalamic acid (NPA), an inhibitor of polar auxin transport, in *nov-1*. In untreated plants, both leaf blades and petioles were significantly shorter in *nov-1* when compared with the wild type (cf. Figure 5C with 5A; see Supplemental Table 1 online). The exogenous application of NPA exacerbated the difference in petiole length between the wild type and *nov-1* (cf. Figures 5D to 5F with 5B). While leaf petioles of wild-type plants treated with NPA were shorter than those of untreated plants (Figures 5A and 5B; see Supplemental Table 1 online), in most *nov-1* plants after NPA application (20/24 plants examined), the petiole was not recognizable (Figures 5D to 5F; see Supplemental Table 1 online). After NPA application, the fusion of rosette leaves was infrequently seen in wild-type plants (8/95 plants examined). In *nov-1*, however, fusion of rosette leaves was significantly induced (64/64 plants examined) (Figures 5D to 5F). In the wild type, NPA application greatly induced the formation of vascular strands in the leaf lamina and petioles, and pronounced unbroken vascular strands extended along the entire margin of the leaf lamina (Mattsson et al., 1999; Figure 5K). By contrast, in *nov-1*, increased formation of vascular strands did not occur, but rudimentary isolated vascular strands were discontinuously formed only in the marginal regions (Figure 5L).

In wild-type roots, NPA induces cell fate changes in epidermal and cortical cells, for example, inducing the development of starch-containing amyloplasts and a broadening of the columella domain (Sabatini et al., 1999; Blilou et al., 2005; Figure 2E). NPA treatment also increases vascular formation in the stele (Mattsson et al., 1999; Sabatini et al., 1999; cf. Figure 5I with 5G). In *nov-1*, cell fate changes in epidermal and cortical cells were much less pronounced, and broadening of the columella domain was repressed (Figure 2F). Furthermore, increased formation of vascular strands was strongly repressed or not seen (cf. Figure 5J with 5H for untreated *nov-1* and with 5I for NPA-treated wild type). Therefore, the *nov-1* mutation does not simply enhance the effect of NPA. When polar auxin transport is inhibited in *nov-1* by NPA, certain aspects of the NPA-induced phenotype are enhanced, such as leaf organ fusion and the suppression of leaf petiole elongation. On the other hand, other aspects, such as NPA-induced vascular formation and root cell fate changes, are strongly repressed. These observations support the hypothesis that *NOV* is required for cell specification and patterning events associated with polar auxin transport.

Formation of Provascular Cells for the Midvein in Leaf Primordia

In wild-type plants, PIN1 expression in leaf provascular cells was first detected close to the center of young primordia, aligned toward the hypocotyl (Figures 6A and 6C). At the apical end of the provascular PIN1 expression domain, almost isodiametric cells exhibited nonpolar or less polar localization of PIN1 with more or less enhanced basal localization (Figure 6A, asterisks; see Supplemental Figure 8 online). A gradual shift from nonpolar to basal localization of PIN1 was observed from the apical to basal side of the midvein provascular strand, which accompanied gradual cell elongation and differentiation into procambial cells (Figures 6A and 6C). These observations raise the possibility that the apical isodiametric cells have progenitor cell–like properties and divide transversely to produce apical daughter cells to be self-maintained as vascular progenitor cells and basal daughter cells to mature into provascular cells. In this scenario, as leaf primordia grow and increase in cell number along the apical-basal axis, the putative vascular progenitor cells should divide transversely. Using 4',6-diamidino-2-phenylindole (DAPI), which allows detection of condensed nuclear DNA in the M phase, and *cyclin B1 promoter:cyclin B1 destruction box:β-glucuronidase* (*CycB1pro:CDB:GUS*), which marks the late G2 to M phase of cell cycle (Colón-Carmona et al., 1999), activity of cell division was examined in 3-d-old wild-type leaf primordia. Cell division activity was detected in the putative vascular progenitor cells for the midvein

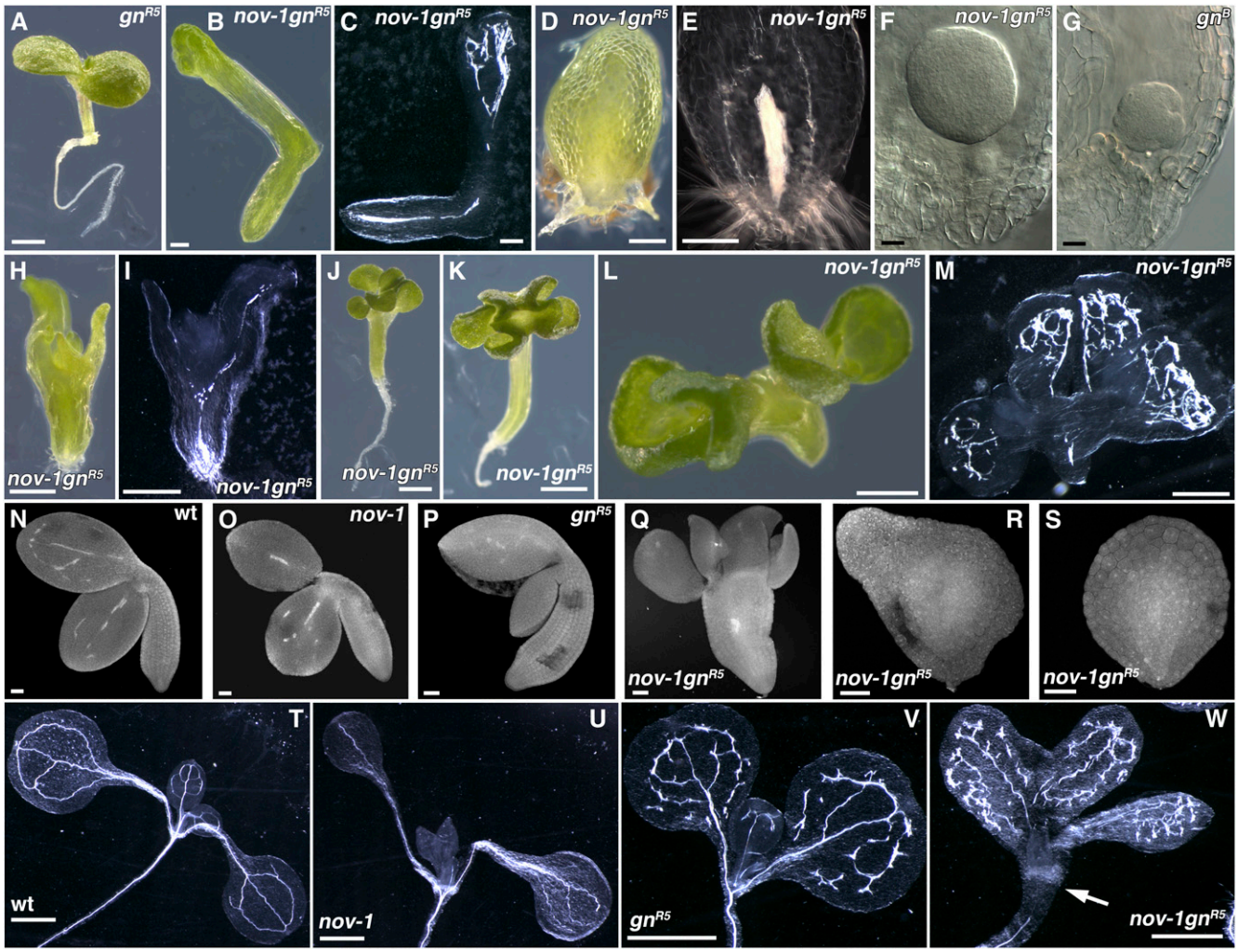

Figure 4. Embryonic and Seedling Phenotype in the *nov-1 gnom*^{R5} Double Mutant.

Embryonic and seedling phenotype in the wild type (**[N]** and **[T]**), *nov-1* (**[O]** and **[U]**), weak allele *gnom*^{R5} (**[A]**, **[P]**, and **[V]**), strong allele *gnom*^{B} **(G)**, and *nov-1 gnom*^{R5} (**[B]** to **[F]**, **[H]** to **[M]**, **[Q]** to **[S]**, and **[W]**). Samples were taken from seedlings (**[A]** to **[E]**, **[H]** to **[M]**, and **[T]** to **[W]**), developing ovules (**[F]** and **[G]**), and imbibed seeds (**[N]** to **[S]**). *nov-1 gnom*^{R5} is shown with either strong phenotype (**[B]** to **[F]**, **[H]** to **[M]**, and **[Q]** to **[S]**) or a relatively weak phenotype **(W)**. Samples in **(B)**, **(D)**, **(H)**, and **(L)** were cleared and shown in **(C)**, **(E)**, **(I)**, and **(M)**, respectively. *nov-1 gnom*^{R5} with strong phenotype failed to develop the primary root (**[B]** to **[F]**, **[H]**, **[I]**, **[L]**, **[M]**, and **[R]**), cotyledons (**[D]** to **[F]**, **[R]**, and **[S]**), and, in some cases, developed multiple cotyledons either fused or not (**[H]** to **[M]** and **[Q]**). In *nov-1 gnom*^{R5} with a weak phenotype, development of lignified xylem strands is repressed at the cotyledon-hypocotyl junction (an arrow in **[W]**). *gn*^{R5}, *gnom*^{R5}; *gn*^{B}, *gnom*^{B}. Bars = 1 mm in **(A)**, **(J)**, **(K)**, and **(T)** to **(W)**, 0.2 mm in **(B)** to **(E)**, 20 μm in **(F)** and **(G)**, 0.5 mm in **(H)**, **(I)**, **(L)**, and **(M)**, and 50 μm in **(N)** to **(S)**.

(Figure 7). DAPI staining allows us to predict the orientation of division plane as judged by direction of alignment of DAPI-stained condensed nuclear DNA. Ten out of the 11 division planes were transverse (Figures 7A and 7B). A transverse division plane accumulating PIN1 protein was also detected (Boutté et al., 2005; Figure 6A, arrow). These results suggest that cells at the apical end of midvein provascular cells have potential characters of midvein progenitor cells.

In epidermal cells of *nov-1* leaf primordia, PIN1 is expressed and localized apically as in the wild type (Benková et al., 2003; Reinhardt et al., 2003; Figures 6B and 6D). Cells with opposite PIN1 polarity were also detected in the epidermis, suggesting that the convergence point of auxin flow is present in *nov-1* leaf primordia. However, provascular PIN1 expression was impaired in *nov-1*, leading to the complete loss of provascular PIN1 expression (Figure 6B). Only in the tip region of leaf primordia was subepidermal PIN1 expression detected, in cells that elongated along the apical-basal axis with apical PIN1 polarity (Figure 6B). When PIN1 expression was detected in provascular cells (Figure 6D), cell elongation occurred much closer to the apical side compared with the wild type (Figure 6C), suggesting precocious vascular differentiation. The most apical provascular

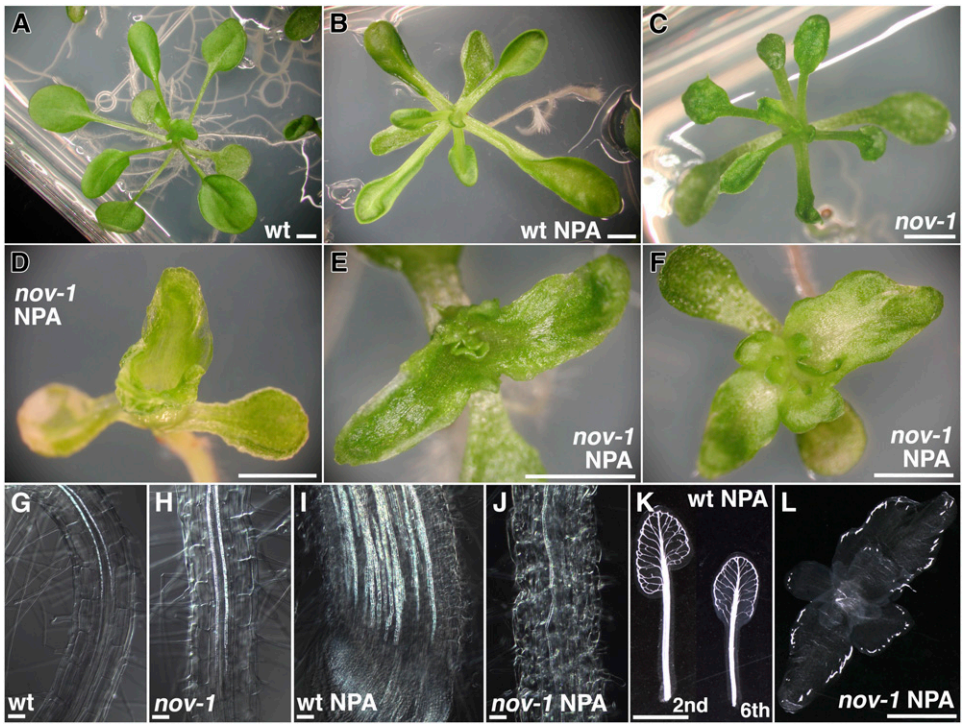

Figure 5. Phenotype of *nov-1* Seedlings Treated with NPA.

(A) to **(F)** Aerial tissue phenotype. Wild type **(A)** and *nov-1* **(C)** grown in the absence of NPA. The wild type **(B)** and *nov-1* (**[D]** to **[F]**) grown in the presence of NPA.

(G) to **(J)** Root vascular tissue phenotype. In roots, increased formation of vascular strands seen in NPA-treated wild-type roots **(I)** is strongly repressed or abolished in *nov-1* **(J)**. Images in **(G)** to **(J)** are regions of cleared roots where the protoxylem cells have started to become lignified.

(K) and **(L)** Leaf vascular tissue phenotype. Shown in **(K)** are cleared samples of the second and sixth rosette leaves of the NPA-treated wild type. The NPA-treated *nov-1* seedling in **(F)** was trimmed cotyledons, cleared and shown in **(L)**. Seedlings were grown in the absence (**[A]**, **[C]**, **[G]**, and **[H]**) or presence of NPA (**[B]**, **[D]** to **[F]**, and **[I]** to **[L]**) for 21 d. The wild type (**[A]**, **[B]**, **[G]**, **[I]**, and **[K]**) and *nov-1* (**[C]** to **[F]**, **[H]**, **[J]**, and **[L]**).

Bars = 2 mm in **(A)** to **(F)**, **(K)**, and **(L)** and 50 μm in **(G)** to **(J)**.

cells also elongated. Basal localization of provascular PIN1 was more or less repressed. Ectopic expression of PIN1 with apical polarity was found in the apical region of the ground tissue (Figures 6B and 6D).

As leaf primordia develop in the wild type, PIN1 is expressed in the looped secondary and tertiary provascular tissues, as well as to a lesser extent in the midvein provascular tissue (Scarpella et al., 2006; Figures 6E and 6I). At this stage, PIN7 was expressed in the region apically adjacent to the distal end of the midvein provascular strand and the region around the border of differentiating midvein procambial cells (Figures 6E and 6F), suggesting that PIN7 plays a role in auxin flow into provascular tissue. In *nov-1* at the corresponding stage, we detected both leaf primordia without provascular PIN1 expression and leaf primordia with a rudimentary provascular PIN1 expression domain in the basal region of leaf primordia (Figures 6G and 6J). Leaf primordia without a PIN7 expression domain apically adjacent to the distal end of the midvein provascular strand were also seen in *nov-1* (Figures 6G and 6H). Taken together, these results suggest that *NOV* is required from the initial stage of provascular formation and throughout the gradual differentiation of provascular cells. Furthermore, *NOV* is required for the development of surrounding ground tissues and, therefore, indirectly regulates auxin flow in developing leaf primordia.

Expression and Subcellular Localization of PIN Proteins Are Altered in *nov-1* Root Tips

The requirement of *NOV* for the correct expression and polarity of PIN proteins was also tested in roots. In contrast with leaf primordia, in roots, no obvious difference in expression and polarity of PIN1 was detected between the wild type and *nov-1* (Figures 6K, 6L, and 6Q to 6T). However, expression and polarity of other PIN members were affected in *nov-1*. In wild-type root tips, PIN2 is polarized apically in the epidermis and basally in the cortex (Friml et al., 2004; Figure 6K). In *nov-1*, PIN2 polarity in the cortex was not basal, but apical or nonpolar (Figure 6L). In the epidermis, PIN2 polarity was apical both in the wild type and *nov-1*. These indicate that *NOV* is essential for basal PIN2 polarity in the cortex but not for apical polarity in the epidermis. In the wild type, expression of PIN3 and PIN7 in columella cells is detected in tiers two and three of columella cells (Blilou et al., 2005; Paponov et al., 2005; Figures 6M, 6Q, and 6S). In *nov-1*, expression of PIN3 and PIN7 in these columella

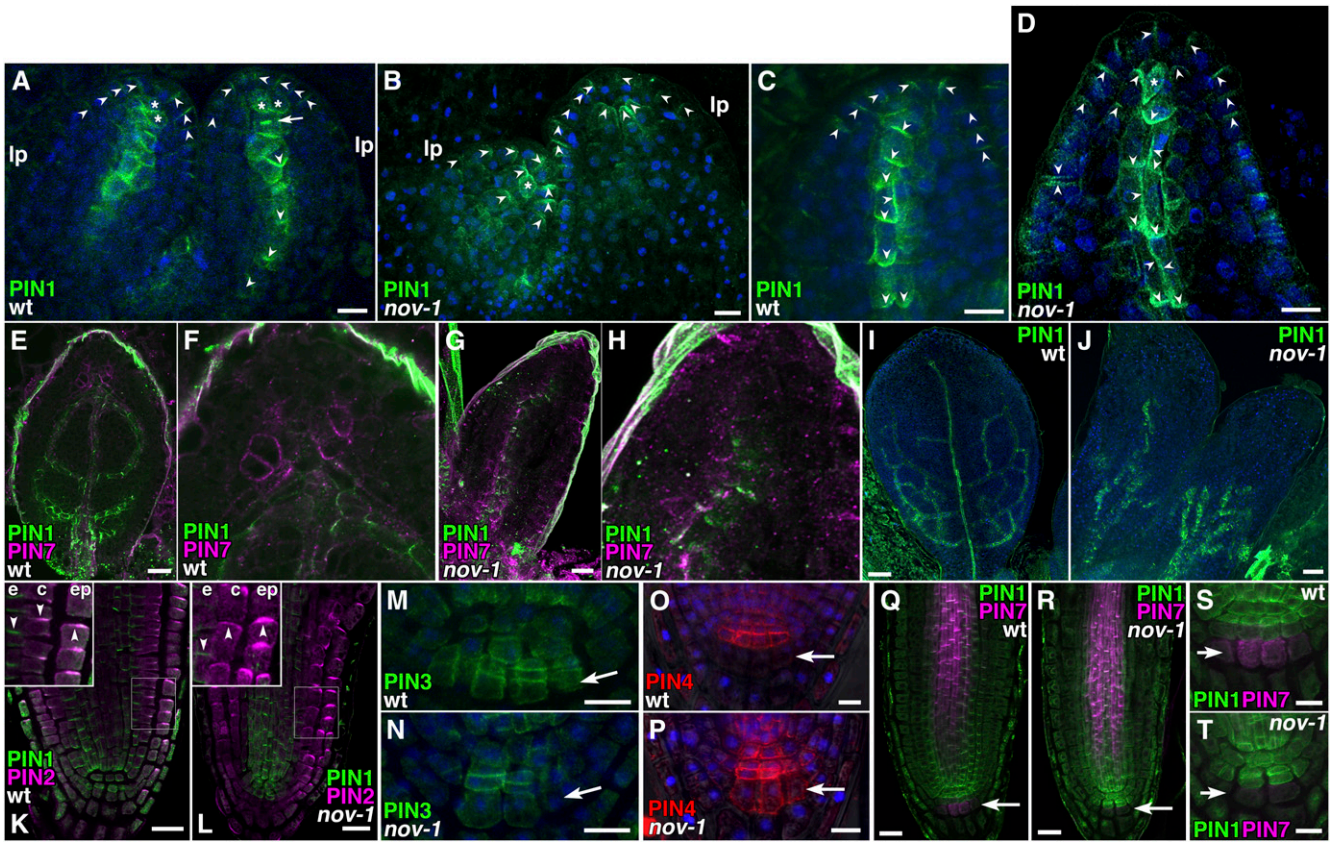

Figure 6. PIN Expression and Localization in the Wild Type and *nov-1*.

(A) to **(J)** Immunostaining of PIN1 and PIN7 in leaf primordia. PIN1 (green in **[A]** to **[J]**), PIN7 (magenta in **[E]** to **[H]**) and DAPI (blue in **[A]** to **[D]**, **[I]**, and **[J]**). Images were obtained from the first two leaf primordia of the wild type (**[A]**, **[C]**, **[E]**, **[F]**, and **[I]**) and *nov-1* (**[B]**, **[D]**, **[G]**, **[H]**, and **[J]**). Asterisks indicate cells with nonpolar PIN1. An arrow in **(A)** indicates PIN1 accumulation at a transverse cell division plane. lp, leaf primordium.

(K) and **(L)** Immunostaining of PIN1 and PIN2 in the root tip. Double staining of PIN1 (green) and PIN2 (magenta) in root tips of the wild type **(K)** and *nov-1* **(L)**. Insets show boxed areas enlarged. e, endodermis; c, cortex; epi, epidermis.

(M) and **(N)** Immunostaining of PIN3 in the root tip. PIN3 (green) and DAPI (blue) in the root stem cell niche of the wild type **(M)** and *nov-1* **(N)**.

(O) and **(P)** Immunostaining of PIN4 in the root tip. PIN4 (red) and DAPI (blue) in the root stem cell niche of the wild type **(O)** and *nov-1* **(P)**.

(Q) to **(T)** Immunostaining of PIN1 and PIN7 in the root tip. Double staining of PIN1 (green) and PIN7 (magenta) in root tips of the wild type (**[Q]** and **[S]**) and *nov-1* (**[R]** and **[T]**). Arrowheads indicate the polarity of PIN proteins for clarity. Arrows in **(M)** to **(T)** indicate the tier three of columella root cap cells. Bars = 10 μm in **(A)** to **(D)**, **(M)** to **(P)**, **(S)**, and **(T)**, 20 μm in **(E)**, **(G)**, **(K)**, **(L)**, **(Q)**, and **(R)**, and 50 μm in **(I)** and **(J)**.

cells was decreased or almost absent (Figures 6N, 6R, and 6T). In the wild-type columella root cap, PIN4 expression is confined to tiers one and two of columella cells (Friml et al., 2002a; Blilou et al., 2005; Paponov et al., 2005; Figure 6O). In *nov-1*, PIN4 expression was expanded to the third tier of columella cells and possibly to the lateral root cap (Figure 6P). Differences in expression of PIN3, PIN4, and PIN7 in other tissues were not detected between the wild type and *nov-1* (Figures 6Q to 6T for PIN7). Nor was any clear difference found in the polarity of PIN3, PIN4, and PIN7 in any tissues. These data indicate that *NOV* is required for proper cell-specific expression of PIN3, PIN4, and PIN7 in the columella root cap.

NOV Encodes a Novel, Plant-Specific Protein

NOV (At4g13750) was identified by map-based cloning. *NOV* comprises 13 exons and 12 introns (Figure 8A) and encodes a novel protein of a predicted 2729 amino acids. The missense mutation in *nov-1* causes substitution of an amino acid from Pro to Ser, the 855th amino acid from the N terminus (Figures 8A and 8B). Four T-DNA insertion lines were identified: *nov-2*, *nov-3*, *nov-4*, and *nov-5* (Figure 8A). All were allelic to *nov-1*. In *Arabidopsis*, another gene (At1g08300) designated *NO VEIN-LIKE* (*NVL*) was found to encode a protein of 746 amino acids, which is mainly composed of domains similar to the N-terminal (197 to 598) and C-terminal (2507 to 2729) parts of NOV with 72 and 69% sequence similarity (percentage in amino acid identity), respectively. *NOV* homologs were found in other plants, including rice (*Oryza sativa*), soybean (*Glycine max*), castor bean (*Ricinus communis*), and moss (*Physcomitrella patens*; Figures 8B and 8C) but not in animals, insects, yeasts, and bacteria, suggesting that *NOV* is specific to the plant kingdom. Sequence similarity of *Arabidopsis* NOV to other plant NOV homologs is

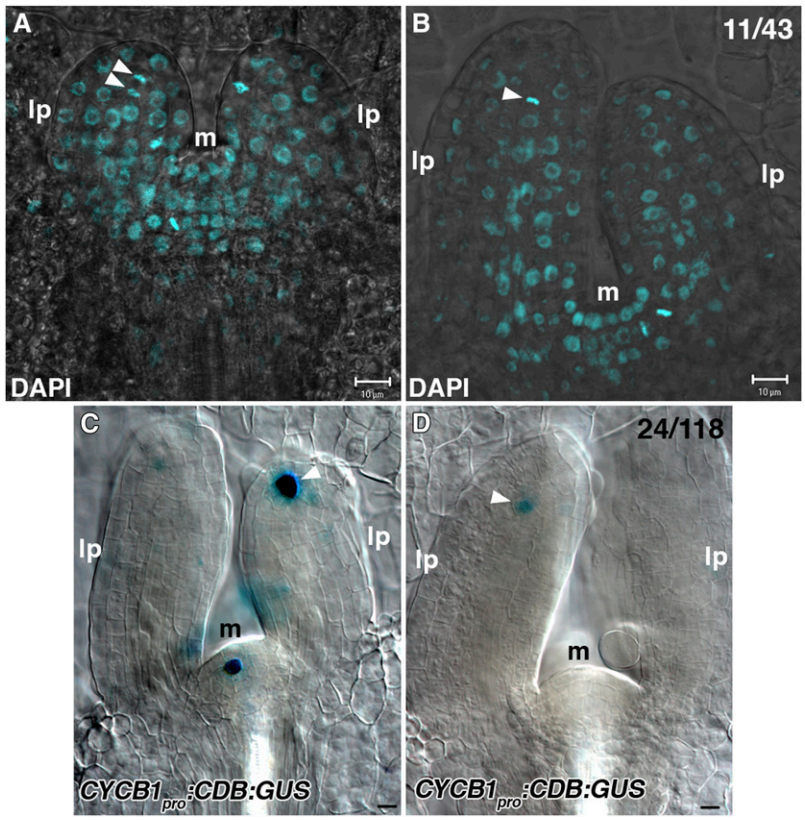

Figure 7. DAPI Staining and *CYCB1*$_{pro}$*:CDB:GUS* Expression in Wild-Type Leaf Primordia.

(A) and **(B)** Wild-type leaf primordia were stained with DAPI. Arrowheads indicate transversely aligned condensed nuclear DNA at the apical ends of provascular cells for the midvein.

(C) and **(D)** The wild type containing *CYCB1*$_{pro}$*:CDB:GUS* was examined for GUS activity. Arrowheads indicate GUS expression at the apical ends of provascular cells for the midvein. All images were taken from the lateral view of leaf primordia. Shown in the top left corner of **(B)** and **(D)** are fractions of primordia with displayed features, respectively.

lp, leaf primordium; m, shoot apical meristem. Bars = 10 μm.

40% to rice NOV (2821 amino acids), 47% to soybean NOV (2711 amino acids), 48% to castor bean NOV (2833 amino acids), and 35% to moss NOV (1962 amino acids). The *Physcomitrella* NOV homolog does not contain a recognizable N-terminal domain. The aforementioned Pro residue, at which substitution to Ser occurs in *nov-1*, is conserved among the plant NOV homologs (Figure 8B). The deduced amino acid sequence of the NOV protein includes a putative GHKL-type-ATPase domain, which has been found in diverse protein families such as DNA gyrase, Hsp90, histidine kinase, and DNA mismatch repair enzyme MutL (Dutta and Inouye, 2000). Figure 8C shows a comparison among the putative GHKL-type-ATPase domains of NOV, plant NOV homologs, protozoan (*Cryptosporidium parvum*) superfamily I helicase and sacsin-like protein, human sacsin and Hsp90-like protein, yeast (*Saccharomyces cerevisiae*) Hsp90, and bacterial (*Rhodopseudomonas palustris*) Hsp90. It must be pointed out that no protein, other than plant NOV homologs and NVL, currently listed in publicly available databases has a significant similarity to NOV. A putative nuclear localization signal (NLS) found in NOV was similar to those that have been experimentally confirmed to be an NLS in human replication factor C subunit 1, chicks DNA topoisomerase 2-β, and fruitfly (*Drosophila melanogaster*) origin recognition complex subunit 2 (http://cubic.bioc.columbia.edu/services/predictNLS/; Figure 8D).

NOV Is a Nuclear Protein and Specifically Expressed in Developing Organs

We created transgenic plants in which *NOV:GFP*, *NOV:GUS*, and *GFP:NOV* translational fusion genes are expressed under control of the *NOV* promoter. *NOV*$_{pro}$*:NOV:GFP* and *NOV*$_{pro}$*:GFP:NOV* were able to complement *nov-1* and *nov-3*, indicating that NOV:GFP and GFP:NOV are functional. Both NOV:GFP (Figures 9, 10B, 10C, and 10I to 10N) and GFP:NOV (see Supplemental Figure 9 online) were specifically localized in the nucleus, with GFP fluorescent signals of higher intensity detected as speckles within the nucleus and the nucleolus, suggesting that NOV is a nuclear protein and may be localized to a specific subnuclear structure.

To clarify further NOV function, the NOV expression pattern was analyzed. In shoots, NOV was expressed in developing leaf

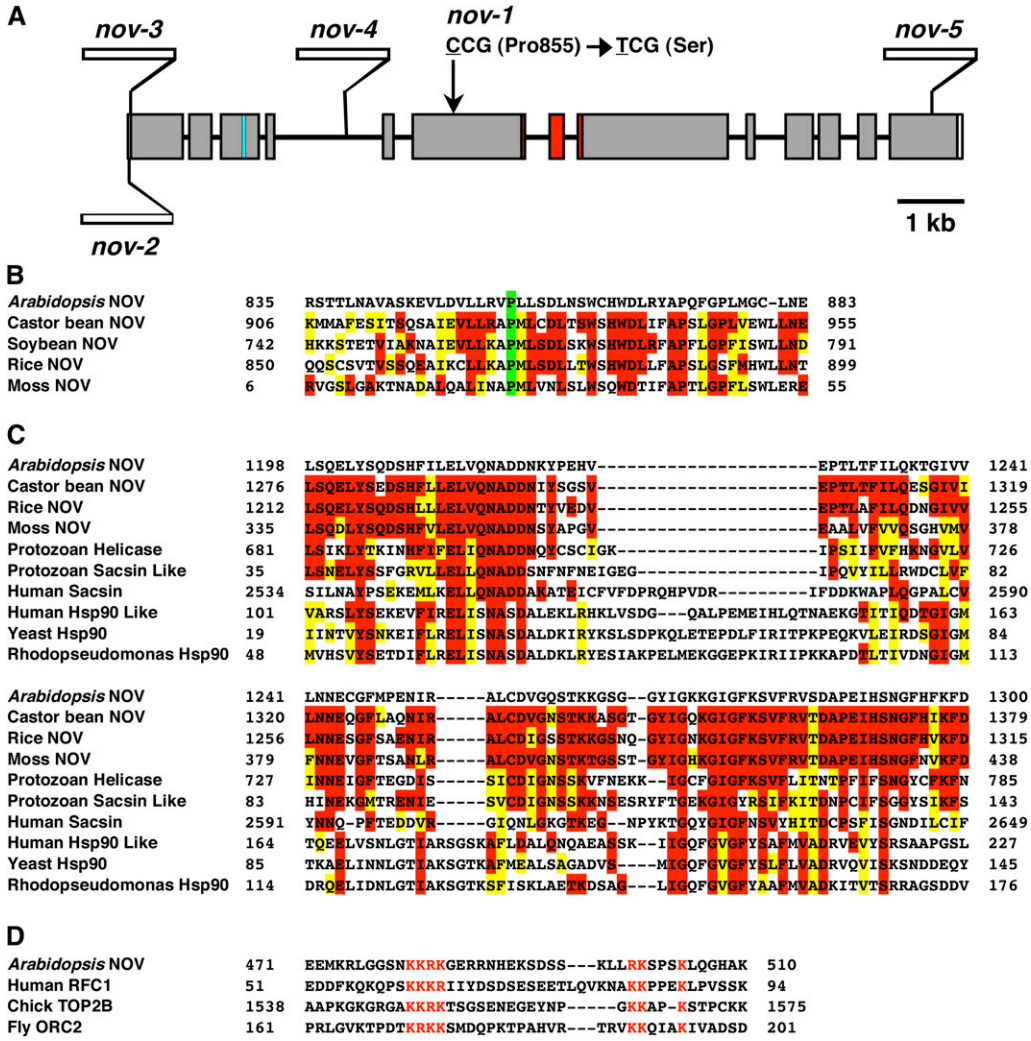

Figure 8. Schematic Structure of *NOV* Gene and Some Features of NOV Protein.

(A) *NOV* gene is composed of 13 exons and 12 introns. The missense mutation site in *nov-1* is schematically indicated by an arrow. Sites of T-DNA insertions in *nov-2*, *-3*, *-4*, and *-5* are shown. Regions coding the putative NLS and the putative GHKL-type ATPase domain are marked in blue and in red, respectively.

(B) Alignment of protein sequences around the 855th Pro residues (marked in green) of NOV homologs. The Pro residue is conserved among NOV homologs in *Arabidopsis*, castor bean, soybean, rice (*O. sativa* Japonica group), and moss.

(C) Comparison of the putative GHKL-type ATPase domain in plant NOV homologs, *Cryptosporidium parvum* superfamily I helicase (Protozoan Helicase), sacsin-like protein (Protozoan Sacsin Like), human sacsin (Human Sacsin), Hsp90-like TNF receptor-associated protein 1 (Human Hsp90 Like), yeast Hsp90 (Yeast Hsp90), and *R. palustris* Hsp90 (Rhodopseudomonas Hsp90). In **(B)** and **(C)**, residues of amino acids identical and similar to those of *Arabidopsis* NOV are marked in red and in yellow, respectively.

(D) The putative NLS in NOV is compared with those that are experimentally confirmed to be a NLS in human replication factor C subunit 1 (RFC1), chicks DNA topoisomerase 2-β (TOP2B), and *Drosophila* origin recognition complex subunit 2 (ORC2). Amino acid residues marked in red are core sequences of K[RK]{3,5}x{11,18}[RK]Kx{2,3}K motif, where K[RK]{3,5} represents for K followed by 3 to 5 of R or K, x{11,18} for 11 to 18 of any amino acid residue, [RK]K for R or K followed by K and x{2,3}K for two to three of any amino acid residues followed by K.

primordia and weakly in the shoot apical meristem (Figures 10A to 10F). This expression pattern is supported by a recent comprehensive study of gene expression in the *Arabidopsis* shoot apical meristem stem cell niche (Yadav et al., 2009). NOV was initially expressed throughout young leaf primordia (Figures 10B and 10C). As leaf primordia develop, NOV expression became restricted to the adaxial side of primordia and then toward the basal side (Figures 10D to 10F). We detected NOV expression in developing embryos and postembryonic NOV expression in provascular cells of cotyledons at the early stage of vascular differentiation (see Supplemental Figure 10 online). In roots, NOV was expressed in the root apical meristem with weak expression in the quiescent center and columella initials but not in mature root tissues (Figures 10A and 10G to 10I). NOV was also

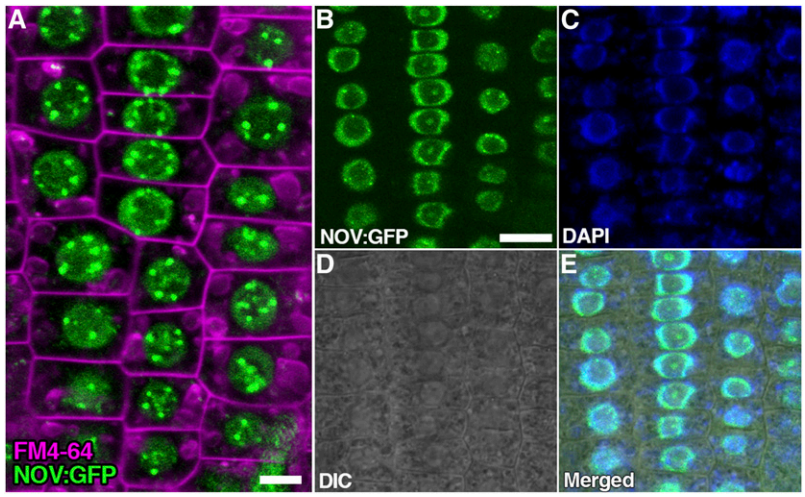

Figure 9. Nuclear Localization of NOV:GFP.

(A) to **(E)** Subcellular localization of NOV:GFP was examined in root epidermal cells of seedlings containing NOV_{pro}*:NOV:GFP* (*NOV:GFP*). Shown in **(A)** is a confocal image of root epidermal cells for NOV:GFP (green) and FM4-64 staining (magenta, plasma and endocytic membranes). NOV:GFP (green in **[B]**), DAPI (blue in **[C]**), differential interference contrast (DIC) optic image **(D)**, and merged image **(E)** are also shown. NOV:GFP is specifically localized in the nucleus. Bars = 5 μm in **(A)** and 10 μm in **(B)** (equal scale in **[B]** to **[E]**).

expressed during primordial development of lateral roots (Figures 10J to 10N). Consistent with the *nov* phenotype, NOV is expressed in developing organs and tissues especially at their early developing and differentiating stages.

DISCUSSION

We have shown here a function, mediated by the *NOV* gene, regulating PIN expression and polarity in a cell type–specific manner. *nov* mutations affect many aspects of auxin-dependent development without directly affecting auxin perception. Our data suggest that *NOV* functions in potentiating cells for competence to undergo auxin-dependent coordinated cell specification and patterning, thereby establishing expression and polarity of PIN proteins.

The Role of *NOV* in Auxin-Mediated Vascular Formation

Epidermal auxin convergence at the tip of an incipient primordium precedes primordium outgrowth (Reinhardt et al., 2000; Heisler et al., 2005). After this convergence, auxin is thought to be channeled from the marginal epidermis into internal tissues in a process that triggers PIN1 expression and polarization in the ground tissue and leads to the formation of provascular cells. This process has also been proposed to instruct the gradual selection of narrow strands of PIN1-expressing provascular cells in developing leaves (Scarpella et al., 2006). Our data indicate that midvein provascular cells become progressively more differentiated toward the basal side of leaf primordia. Relatively isodiametric cells with nonpolar PIN1 at the apical end of the midvein provascular strand divide transversely, stacking daughter cells along the apical-basal axis. A new basal daughter cell therefore abuts both a new apical daughter cell and an older basal daughter cell, which has already initiated gradual basal polarization and differentiation. Thus, in addition to the auxin gradient, the automatic placement of new basal daughter cells into an existing cell polarity gradient may contribute to its position-dependent polarity. It may also serve to initiate developing vascular cells' gradual differentiation, connecting production of preprocambial cells with their polarity acquisition and continuity. These data suggest that the cells with nonpolarly localized PIN1 in the tip of leaf primordium are progenitor cells for the midvein. This environment with an auxin maximum resembles that of the root stem cell niche, although the auxin flow is topologically opposite.

It has been recently reported that, before leaf primordia bulge out from the surface of the meristem, subepidermal PIN1 is transiently polarized toward the PIN1 convergence point in the epidermis in a process that could underlie the formation of the auxin maximum at the tip of the incipient primordium (Bayer et al., 2009). Subsequently, in bulging leaf primordia, midvein provascular cells with basal PIN1 polarity emerge. In *nov-1* leaf primordia, subepidermal PIN1 expression and polarity are impaired to such an extent that provascular PIN1 expression is completely missing, and though PIN1 in the apical subepidermal region is apically polarized, epidermal PIN1 expression and polarity remain normal. Consistent with these data, in *nov-1* leaf primordia, *DR5* expression tends to be confined to the marginal epidermis, especially at the tip. Furthermore, the first two rosette leaves in *nov-1* were occasionally observed entirely without veins. These leaves developed from primordia without provascular tissues (as judged by expression of *J1511-GFP* and *ATHB8*). It is worth noting here that the apical polarity of subepidermal PIN1 in *nov-1* primordia is topologically similar to the aforementioned apical polarity of subepidermal PIN1 seen in wild-type incipient primordia before they express PIN1 in provascular cells. Our observations suggest that *NOV* is required for provascular PIN1

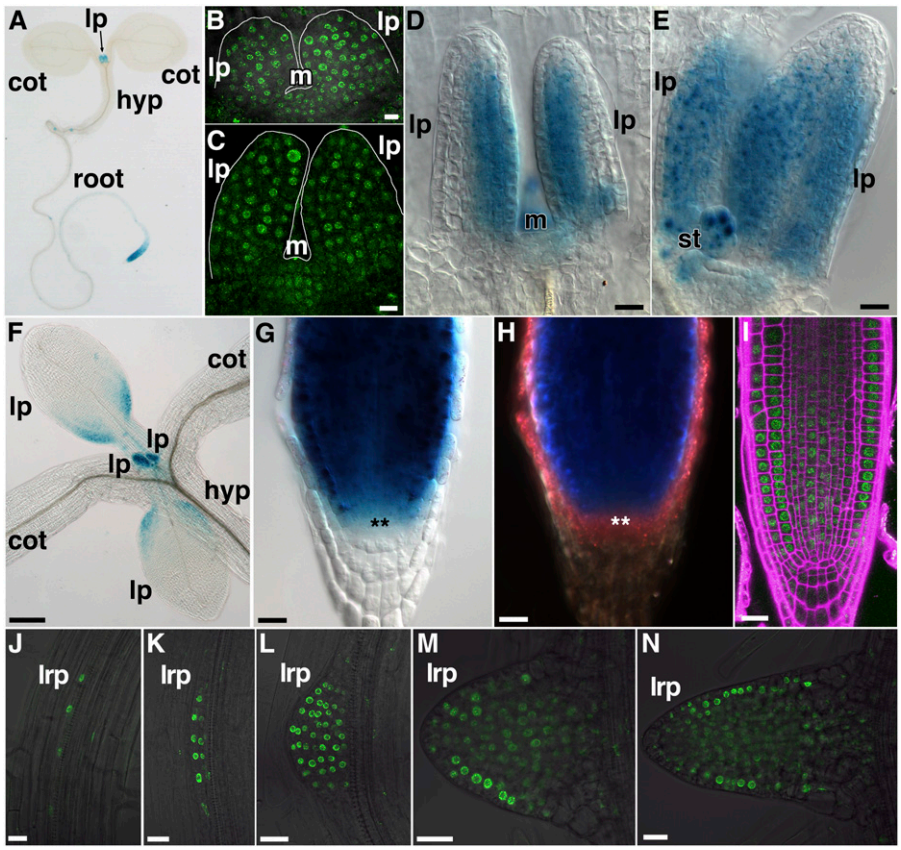

Figure 10. Expression of *NOV* in Seedlings, Leaf Primordia, and Roots.

(A) to **(F)** Expression of NOV_{pro}*:NOV:GUS* (**[A]** and **[D]** to **[F]**) and NOV_{pro}*:NOV:GFP* (**[B]** and **[C]**) in seedlings. A whole seedling **(A)** and leaf primordia (**[B]** to **[F]**). Images in **(B)** to **(D)** were taken from the lateral view of leaf primordia. Leaf primordia shown in **(A)** to **(E)** and in **(F)** are of the first and second rosette leaves and of the first to fourth rosette leaves, respectively.

(G) to **(N)** Expression of NOV_{pro}*:NOV:GUS* (**[G]** and **[H]**) and NOV_{pro}*:NOV:GFP* (**[I]** to **[N]**) in roots. Primary root tips (**[G]** to **[I]**) and lateral root primordia (**[J]** to **[N]**). **(H)** is a dark-field image of the sample in **(G)**. In **(G)** and **(H)**, cells of the quiescent centers are marked by asterisks. The root tip in **(I)** was stained with propidium iodide (magenta) for detecting cell boundary. Samples were taken from seedlings grown for 3 d **(B)**, 3.5 d **(C)**, 4 d **(A)**, 5 d (**[D]**, **[E]**, and **[I]**), 7 d (**[F]** to **[H]** and **[L]** to **[N]**), and 8 d (**[J]** and **[K]**) after germination. cot, cotyledon; hyp, hypocotyl; lp, leaf primordium; lrp, lateral root primordium; m, shoot apical meristem; st, stipule.

Bars = 10 μm in **(B)**, **(C)**, and **(J)** to **(N)**, 20 μm in **(D)**, **(E)**, and **(G)** to **(I)**, and 0.2 mm in **(F)**.

expression and polarization in the ground meristem after an auxin convergence point is formed in the epidermis at the tip of an incipient primordium. Furthermore, subsequent termination of leaf provascular formation and repressed basal polarization of midvein provascular PIN1 also appear to occur in *nov-1*. In *nov-1* and *nov-3* leaves, ground tissue cells, where the vascular path might be predicted in the wild type, either do not include elongated vascular cells or include elongated cells with or without differentiated xylem cells (see Supplemental Figure 11 online). These data suggest that *NOV* is required for provascular formation throughout leaf primordial development for the proper differentiation of provascular cells and their development into xylem cells. This hypothesis is further supported by the fact that *NOV* is postembryonically expressed in provascular cells of cotyledons at early stages of vascular differentiation.

In *nov-1*, the 2,4-D–induced lateral root failed to develop vascular cells despite the presence of a functional auxin response. When grown in the presence of NPA, an inhibitor of polar auxin transport, the increased formation of vascular tissue seen in leaves and roots of wild-type seedlings is greatly repressed in *nov-1*, although organ fusion is greatly enhanced. *NOV* is also required for early provascular development during embryogenesis. These results suggest that *NOV* facilitates cells' acquisition and maintenance of the competence to differentiate into vascular cells in response to auxin. We therefore suggest that in leaf primordia, *NOV* establishes provascular expression and polarity of PIN1.

Vascular continuity is achieved through reiterative coordinated cell polarization for provascular development. Vascular continuity defects seen in $gnom^{R5}$ are enhanced in *nov-1* $gnom^{R5}$ seedlings, further indicating that *NOV* is important for vascular development. GNOM is directly involved in regulated intracellular vesicle trafficking of PIN1 (Geldner et al., 2003), a function that is considered to be instrumental for the coordinated polarization of PIN1 (Steinmann et al., 1999; Geldner et al., 2004; Kleine-Vehn

et al., 2008a). Therefore, it is likely that in *nov-1 gnom^{R5}*, auxin-mediated vascular development is synergistically impaired both by a decreased competence of cells for vascular differentiation due to the *nov-1* mutation and by defective coordinated polarization of PIN1 due to the *gnom^{R5}* mutation.

The Role of *NOV* in Auxin-Mediated Organ Formation during Embryonic and Leaf Development

It has been shown that efflux-dependent auxin gradients are required for apical-basal patterning during embryonic development and that both the *pin7* mutation and NPA treatment disrupts the apical-basal pattern of auxin distribution in the embryo, giving an ectopic auxin response in the suspensor (Friml et al., 2003). *nov-3* embryos, whose phenotype is similar to those of mutants defective in efflux-dependent polar auxin transport (Steinmann et al., 1999; Friml et al., 2003; Vieten et al., 2005), exhibit an ectopic auxin response in the tips of cotyledon primordia and in the suspensor. These suggest that efflux-dependent auxin gradients are impaired in embryos of strong *nov* alleles, *nov-2*~*5*. Thus, *NOV* may be required for establishment of PIN expression and polarity during embryonic development.

Expression of *J1511-GFP* was impaired in *nov-1* leaf primordia and *nov-5* embryos. In the J1511 line, an enhancer-trap T-DNA (Laplaze et al., 2005) was found to be inserted in an intergenic region between At1g19840 (11.4 kb away) and At1g19850 (2.1 kb away). At1g19840 encodes an auxin-responsive family protein and At1g19850 encodes MONOPTEROS (MP). In fact, the spatial distribution of *J1511-GFP* expression is similar to that of *MP* mRNA (Hardtke and Berleth, 1998; Hardtke et al., 2004; Wenzel et al., 2007). During embryogenesis, *J1511-GFP* is almost uniformly expressed from the mid to late globular stages (see Supplemental Figure 12A online). The expression starts to become restricted to the central region from around the heart stage (Figures 3D and 3I; see Supplemental Figure 12B online) and is then confined to the provascular tissue and root cap at later stages of development (Figure 3J; see Supplemental Figures 12C and 12D online). These data suggest that the expression of *J1511-GFP* may reflect that of *MP*, which is known to partially regulate the provascular expression of PIN1 in the leaf primordium (Wenzel et al., 2007). It was previously reported that a strong loss-of-function *mp* mutant, *mpG12*, exhibits no cotyledon growth and has discontinuous vascular strands and that *MP* antisense lines have fewer higher order veins in rosette leaves (Hardtke et al., 2004). *nov-5* embryos devoid of cotyledon do not express *J1511-GFP* in the apical part of embryos. *nov-5* embryos with some outgrowth of cotyledons exhibit *J1511-GFP* expression in the apical part, although provascular *J1511-GFP* expression tends to be missing or strongly repressed. *nov-1* leaf primordia also exhibit loss of provascular *J1511-GFP* expression. Thus, if expression of *J1511-GFP* reflects that of *MP*, *NOV* function may partly underlie the establishment of *MP* expression, thereby supporting provascular development in cotyledons and leaf primordia.

In *nov-1 gnom^{R5}* embryos and seedlings, apical-basal patterning defects, including complete loss of the cotyledon and/or root, are seen. The same phenotype classes are also seen in strong *gnom* alleles (Mayer et al., 1993). GNOM directly regulates the polar localization of PIN1 and therefore controls auxin distribution. This report establishes that *NOV* plays an important role in directing PIN expression and polarity through cell fate decisions. We hypothesize that, although each weak mutation causes relatively mild effects on embryonic development, when combined in *nov-1 gnom^{R5}* embryos, auxin distribution is synergistically impaired to the extent that apical-basal patterning is severely disrupted in a similar manner to that seen in strong *gnom* alleles, where coordinated PIN1 polarity for embryo axis formation is severely disrupted (Steinmann et al., 1999).

In addition to cotyledon growth, separation of cotyledon primordia are repressed in *nov-2*~*5* embryos. When grown in the presence of the polar auxin transport inhibitor NPA, even in the weak *nov-1* allele, leaf organ separation is repressed. It has been suggested that auxin distribution in the apical part of the embryo is important for cotyledon separation (Furutani et al., 2004). 2,4-D treatment causes broader distribution of auxin in the developing embryo (Friml et al., 2003) and induces cotyledon fusion (Furutani et al., 2004). Separation of shoot-derived lateral organs is associated with a local reduction of auxin, which may be induced by divergence of auxin flow (Heisler et al., 2005). In *nov-1* leaf primordia and *nov-3* cotyledon primordia, as provascular development is impaired, one might expect that auxin is not efficiently drained through the primordium. Thus, as ectopic epidermal *DR5* expression is detected in *nov-1* leaf and *nov-3* cotyledon primordia, a broader auxin distribution would be expected to form in the apical regions of leaf and cotyledon primordia of *nov* mutants. This may enhance the inhibitory effect of NPA on the separation of lateral organ primordia. Therefore, we think that *NOV* function contributes indirectly to lateral organ separation. A similar scenario may be applied to the multiple-cotyledon phenotype of *nov-1 gnom^{R5}* and *nov-1 gnom$^{B/E}$*, which is neither seen in *nov* nor in *gnom* strong alleles. Broadly increased cellular auxin concentration in the apical part of embryos and enhanced PIN polarity defects in *nov-1 gnom^{R5}* and *nov-1 gnom$^{B/E}$* may increase the probability of multiple auxin maxima forming as cotyledon primordia start to develop, leading to the outgrowth of four to six cotyledons. On the other hand, a contrasting scenario may be applied to the leaf petiole phenotype of *nov-1* treated with NPA. Auxin positively regulates petiole elongation (Pierik et al., 2009). As auxin flow from the apical to basal region of the leaf primordia is synergistically decreased both by impaired provascular development and by chemical inhibition of auxin transport, auxin concentration would be expected to decrease in the basal region of leaf primordia, potentially abrogating auxin-mediated petiole elongation and petiole formation. In summary, whether they are primary consequences of *nov* mutations or their secondary effects, the defects associated with *nov* mutations described here highlight the importance of *NOV* in many aspects of auxin-mediated development.

The Role of *NOV* in Auxin-Mediated Cell Specification and Patterning in Roots

We have shown that *NOV* is required for auxin-mediated cell specification and patterning not only in the leaf, but also in the root. It has been shown that *SCR* (Sabatini et al., 2003), *PLT* (Aida et al., 2004), and *WUSCHEL-RELATED HOMEOBOX5* (Sarkar et al., 2007) control stem cell maintenance in roots and that

regulation of *PLT* expression by the GCN5 histone-acetyltransferase complex is essential for root stem cell maintenance (Kornet and Scheres, 2009). *PLT* genes are considered to be cell fate regulators in auxin-mediated cell specification and patterning, redundantly controlling expression of *PIN* genes in specific domains (Aida et al., 2004; Blilou et al., 2005; Galinha et al., 2007). In the *plt1 plt2* double mutant, *PIN4* mRNA, which is normally expressed in the root tip, is absent. Also, the expression of *PIN3* and *PIN7* mRNA is normal in columella cells, but markedly reduced in the provascular cells of roots (Blilou et al., 2005). A contrasting situation is seen in *nov-1*. Here, expression of PIN4 in columella cells is expanded and encompasses one more outer tier of columella cells, whereas expression of PIN3 and PIN7 is absent or markedly reduced in columella cells, while PIN7 is expressed normally in provascular cells. The strong reduction of PIN3 and PIN7 expression in columella cells of *nov-1* might not simply be due to hastened differentiation of columella cells because differentiation of columella stem cells also occurs in *plt1 plt2* (Aida et al., 2004). An expansion of the PIN4 expression domain may be due to the compensatory mechanism of PIN redundancy (Vieten et al., 2005). It should be noted that, in *nov-1*, in contrast with the internal tissue in leaf primordia, there is no obvious defect in PIN1 expression and polarity in roots. In addition, PIN7 expression in columella cells and the region immediately distal to the leaf midvein provascular strand is strongly repressed in *nov-1*, while the PIN7 expression persists along the differentiating procambium in the leaf and root. These data suggest regional specificity for the requirement of *NOV* control over the expression of PIN1 and PIN7, as well as for PIN1 polarity.

A basal-to-apical shift in polarity of PIN2 is observed in the root cortex of *nov-1*. A similar polarity defect of PIN2 in the root cortex is caused also by overexpression of PINOID (PID) protein kinase (Friml et al., 2004) and by loss-of-function mutations in genes encoding protein phosphatase 2A (PP2A) (Michniewicz et al., 2007). However, *PID* overexpression and *PP2A* mutations result in basal-to-apical shifts not only for PIN2 in the cortex but also for PIN1 and PIN4 in their respective expression domains. PID and PP2A both partially colocalize with PINs and antagonistically regulate apical-basal localization of PINs (Michniewicz et al., 2007). On the other hand, in *nov-1*, the basal-to-apical shift was detected only for PIN2 in the cortex. NOV, as a nuclear protein, does not colocalize with PINs and is therefore unlikely to directly influence their polarity. It is of course possible that NOV controls the expression of factors that do control PIN polarity, possibly including PID and PP2A.

PLT, *SCR*, and *SHR* genes appear to regulate indirectly expression of *PIN* genes through determination or stabilization of cell fate in the root meristem (Sabatini et al., 2003; Aida et al., 2004; Blilou et al., 2005; Xu et al., 2006). Our data suggest that *NOV* also indirectly regulates expression and polarity of PIN proteins through mechanisms that include the determination and/or stabilization of cell fate in the root meristem.

NOV Mediates Cell Acquisition of the Competence to Undergo Auxin-Mediated Cell Specification and Patterning in the Embryo, Shoot, and Root

Local, efflux-dependent auxin gradients have emerged as a unifying mechanism underlying plant organ formation (Benková et al., 2003). The auxin-efflux pattern is regulated by dynamic expression and asymmetric subcellular localization of PIN auxin-efflux proteins during plant organogenesis (Benková et al., 2003; Friml et al., 2003; Reinhardt et al., 2003; Blilou et al., 2005; Scarpella et al., 2006; Bayer et al., 2009). Thus, the question of how the expression and subcellular localization of PIN proteins are controlled goes to the heart of plant development. We have shown here that (1) *NOV* is required for PIN expression and polarity in a cell type–specific manner, for provascular PIN1 expression and region-specific expression of PIN7 in leaf primordia, for cell type–specific expression of PIN3, PIN4, and PIN7 in the root stem cell niche, and for PIN2 polarity in the root cortex. (2) *NOV* helps cells to acquire and maintain their ability to differentiate into vascular cells in response to auxin. (3) *NOV* is required for normal cellular organization and stem cell maintenance in the root stem cell niche. (4) *NOV* has an important role in auxin-mediated embryonic development. (5) *NOV* function may partly underlie establishing *MP* expression for growth of cotyledon primordia and provascular development in cotyledon and leaf primordia. (6) *NOV* encodes a plant-specific nuclear factor specifically expressed in developing organs and tissues. From the data presented in this report, we propose that *NOV* is a competence factor for auxin-dependent coordinated cell specification and patterning during plant organ formation. That is, *NOV* is involved in mediating cell acquisition of competence to undergo auxin-dependent polar development, thereby establishing PIN expression and polarity, developmentally regulated auxin distribution, and possibly *MP* expression, all of which are intertwined to form a positive feedback loop for auxin-mediated polar development. What is the cellular and molecular basis for such acquisition of competence? This question remains unanswered, but knowledge of the biochemical function of NOV and the relationship of *NOV* with other known cell fate regulators may lead us to an answer. This knowledge will be uncovered by the identification of factors interacting physically with the NOV protein and genetically with the *NOV* gene. Since NOV is a nuclear protein, NOV may act primarily in transcriptional or posttranscriptional regulation of nuclear gene expression. Thus, assessment of transcriptional outputs in *nov* mutants would also be beneficial to understanding the primary function of NOV. Furthermore, future studies on *NOV* may shed new light on the fundamental mechanisms by which auxin regulates the formation of plant organs and tissues, regardless of their fate and origin.

METHODS

Plant Materials and Growth Conditions

Arabidopsis thaliana ecotypes C24, Columbia (Col), and Landsberg *erecta* were used as wild-type controls according to the genetic backgrounds of mutants and plant lines. The following mutants were used: *nov-1* (C24), *nov-2*, *-3*, *-4*, and *-5* (Col), $gnom^{R5}$ (Landsberg *erecta*), and $gnom^{B/E}$ (Col) (Geldner et al., 2004). *nov-2* (*emb2597*), *nov-3* (salk_096246), *nov-4* (salk_049619), and *nov-5* (salk_028690) were obtained from the ABRC. Marker lines used were J1511 (C24) (from ABRC), $DR5_{pro}$*:GUS* (Col) (Ulmasov et al., 1997), $DR5_{pro}$*:GFP* (Col) (Ottenschläger et al., 2003), $ATHB8_{pro}$*:GUS* (Col) (Baima et al., 1995), $CYCB1_{pro}$*:CDB:GUS* (Colón-Carmona et al., 1999), SHR_{pro}*:GFP* (Col) (Helariutta et al., 2000), and SCR_{pro}*:GFP* (Col) (Wysocka-Diller et al., 2000).

T-DNA insertion alleles, *nov-2*, *-3*, *-4*, and *-5*, were characterized at both ends of each insertion and confirmed to be integrated into the transcriptional unit of *NOV* gene (Figure 8A). As the first nucleotide of the initiator ATG is numbered as +1, insertion positions of *nov-2*, *-3*, *-4*, and *-5* T-DNA are as follows: *nov-2* T-DNA, between −41 (5′ untranslated region) and +12 with 51-bp deletion in the first exon; *nov-3* T-DNA, between +12 and +33 with 20-bp deletion in the first exon; *nov-4* T-DNA, between +3204 and +3211 with 6-bp deletion in the fourth intron; and *nov-5* T-DNA, between +11987 and +12006 with 18-bp deletion in the thirteenth exon. *nov-1*～*5* mutants were backcrossed at least twice, respectively.

For growing plants on plates, seeds were sterilized and plated on agar-solidified basal medium containing 0.5× Murashige and Skoog salts, pH 5.7, 1% sucrose, and 0.7 or 1.5% agar. Before germination, seeds were placed at 4°C in the dark for 3 to 5 d. Plants were grown on horizontally placed 0.7% agar plates or vertically on the surface of 1.5% agar plates. Unless written otherwise, growth temperature is 21 to 22°C. For immunohistochemical detection of PIN proteins, seedlings grown at 27°C were used.

Mutagenesis and Screening

The enhancer-trap line J1511, in which reporter GFP is expressed in the provascular cells, was mutagenized with 0.1% (v/v) ethyl methanesulfonate (Sigma-Aldrich). Leaf vein patterns were observed in living M2 seedlings by detecting GFP expression in the provascular cells under a fluorescent dissection microscope.

Phenotypic Analyses

For observation of venation patterns, dissected leaves or seedlings were fixed in ethanol/acetic acid (6:1). Fixed samples were washed several times in 70% ethanol and then whole mounted in chloral hydrate solution (8 g of chloral hydrate, 1 mL of glycerol, and 2 mL of water). Developing embryos were observed as described previously (Tsugeki et al., 1996). For visualization of starch granules in root tips, roots excised from plants vertically grown for 8 d were incubated in Lugol solution (Sigma-Aldrich) and mounted in the chloral hydrate solution.

GUS Staining

Samples were first placed in ice-cold acetone for 15 min and then in GUS staining solution containing 0.5 mg/mL X-Gluc, 0.1 M sodium phosphate buffer, pH 7.0, 10 mM EDTA, 5 mM potassium ferricyanide, 5 mM potassium ferrocyanide, and 0.1% Triton X-100. Samples in the GUS staining solution were placed under vacuum and incubated either at room temperature (16 to 18 h for *CYCB1*$_{pro}$*:CDB:GUS*, *DR5*$_{pro}$*:GUS* in leaves, and *ATHB8*$_{pro}$*:GUS*) or at 37°C (2 h for *DR5*$_{pro}$*:GUS* in roots and 18 to 24 h for *NOV*$_{pro}$*:NOV:GUS*). Stained samples were processed as described above.

Immunolocalization of PIN Proteins

Samples were fixed and processed as described previously (Gälweiler et al., 1998). Polyclonal antibodies raised against PIN1, PIN2, PIN3, PIN4, and a monoclonal antibody raised against PIN7 were used as primary antibodies. As secondary antibodies, Alexa Fluor 488 goat anti-rabbit IgG and Alexa Fluor 555 anti-mouse IgG were used, respectively. Processed samples were mounted in *SlowFade* Gold antifade reagent with or without DAPI (Invitrogen) and subjected for confocal microscopy.

Microscopy

Images of seedlings were captured on a Leica M420 Macroscope equipped with Nikon COOLPIX 990 or Leica DFC280 digital camera system. GFP fluorescence in living seedlings was detected on the fluorescence dissection microscope MZFLIII (Leica) equipped with a digital camera system (C4742-95; Hamamatsu). Observation of mature embryos by aniline blue staining was performed as previously described (Bougourd et al., 2000). For DAPI staining, fixed samples were stained in 0.2 mg/L DAPI for 15 min, washed three times, and mounted on a glass slide. Optical sections were obtained using a Zeiss Axioplan 2 microscope equipped LSM 5 PASCAL (Carl Zeiss). The 405-nm excitation line of a 25-mW blue diode laser was used, and signals were collected through a band-pass filter of 420 to 480 nm. For confocal microscopy on leaf primordia, fluorescent signals were checked throughout the tested primordia.

Positional Cloning, Plasmid Construction, and Plant Transformation

The F2 population of the F1 hybrid between *nov-1* (C24) and Col was used for mapping. By fine mapping, *NOV* was mapped between At4g13670 and At4g13800. An ～17-kb genomic fragment containing the At4g13750 gene with 3.3-kb upstream and 1.4-kb downstream regions (from 7,971,914 to 7,989,006 bp on chromosome 4) was cloned into pGW-NB1 (Nakagawa et al., 2007). The resulting construct was able to complement *nov-1*, *nov-3*, or *nov-5*. *G3GFP* (Kawakami and Watanabe, 1997) or *GUS* gene was inserted into the aforementioned 17-kb genomic fragment in such a way that translational fusion genes *NOV:GFP*, *NOV:GUS*, and *GFP:NOV* would be expressed under the *NOV* promoter. To determine the exon-intron structure of At4g13750, RT-PCR analysis was performed based on the gene annotation data.

Hormone and Chemical Treatments

Seedlings were incubated either in water containing 10 μM 2,4-D or on agar-solidified medium containing 1 μM 2,4-D. For detecting *DR5*$_{pro}$*:GUS* expression in leaves and roots, seedlings were first grown in the absence of 2,4-D and then incubated with 10 μM 2,4-D for 1 d and with 1 μM 2,4-D for 3 d, respectively. For analysis of 2,4-D–induced lateral roots, seedlings were grown in the presence of 1 μM 2,4-D for 11 d. For NPA treatment, seedlings were grown on agar-solidified medium containing 10 μM NPA for 8 d (starch staining of root tips) and for 21 d (phenotypic analysis in Figure 5).

Accession Numbers

Sequence data from this article can be found in The Arabidopsis Information Resource (http://www.Arabidopsis.org/) or GenBank/EMBL databases under the following accession numbers: NOV, At4g13750; NVL, At1g08300; castor bean (*Ricinus communis*) NOV, EEF44191.1; soybean (*Glycine max*) NOV, AAQ62582.1; rice (*Oryza sativa* Japonica group) NOV, EEE60127.1; moss (*Physcomitrella patens*) NOV, XP_001777863.1; protozoan (*Cryptosporidium parvum*) superfamily I helicase, XP_626083; protozoan Sacsin-like protein, XP_627068; human Sacsin, NP_055178 (Engert et al., 2000); human Hsp90-like protein (TNF receptor-associated protein 1), NP_057376; human replication factor C subunit 1 (RFC1), P35251; yeast (*Saccharomyces cerevisiae*) Hsp90, P02829; *Rhodopseudomonas palustris* Hsp90, ZP_02301386; chicks DNA topoisomerase 2-β (TOP2B), O42131; *Drosophila* origin recognition complex subunit 2 (ORC2), Q24168.

Supplemental Data

The following materials are available in the online version of this article.

Supplemental Figure 1. *ATHB8*$_{pro}$*:GUS* Expression in *nov-1*.

Supplemental Figure 2. Maintenance of Columella Root-Cap Stem Cells Is Defective in *nov-3*.

Supplemental Figure 3. Maintenance of Cortex/Endodermis Stem Cells Is Defective in *nov-3* Root Tips.

Supplemental Figure 4. Abnormality in Formation of Vascular Stem Cells in *nov* Mutants during Embryogenesis.

Supplemental Figure 5. Ectopic Cell Division in the Quiescent Center of *nov-2* during Embryogenesis.

Supplemental Figure 6. Expression of SCR_{pro}*:GFP* and SHR_{pro}*:GFP* in Embryos with Strong *nov* Alleles.

Supplemental Figure 7. Seedling Phenotype in *nov-1* $gnom^{B/E}$ Double Mutant.

Supplemental Figure 8. Subepidermal Cells at the Apical End of the Midvein Provascular Strand Exhibit Nonpolar PIN1 Localization.

Supplemental Figure 9. Nuclear Localization of GFP:NOV.

Supplemental Figure 10. NOV_{pro}*:NOV:GUS* Expression in Embryos and in Cotyledons of Developing Seedlings.

Supplemental Figure 11. Vascular and Ground-Tissue Phenotypes in *nov-1* and *nov-3* Leaves.

Supplemental Figure 12. *J1511-GFP* Expression during Embryogenesis.

Supplemental Table 1. Leaf and Petiole Lengths of the First Two Rosette Leaves of Seedlings Grown in the Absence or Presence of NPA.

ACKNOWLEDGMENTS

We thank Philip Benfey for SCR_{pro}*:GFP* and SHR_{pro}*:GFP*, Peter Doerner for $CYCB1_{pro}$*:CDB:GUS*, Tom J. Guilfoyle for $DR5_{pro}$*:GUS*, Gerd Jürgens for $gnom^{R5}$ and $gnom^{B/E}$, Giorgio Morelli for $ATHB8_{pro}$*:GUS*, Tsuyoshi Nakagawa for pGWB-NB1, Yuichiro Watanabe for *G3GFP*, the ABRC for J1511 and *nov-2*, *-3*, *-4*, and *-5*, Toshiharu Shikanai for critically reading the manuscript, Sumie Ishiguro, Noritaka Matsumoto, and Nana Tanaka for stimulating discussions, and Shiho Terada and Irina Kneuper for technical assistance. This work was supported in part by a Grant-in-Aid for Scientific Research (13740455 and 21657014 to R.T.) from the Japan Society for the Promotion of Science, by a Grant-in-Aid for Creative Scientific Research (19GS0315 to K.O. and R.T.) and a Grant-in-Aid for Scientific Research on Priority Areas (19060004 to K.O.) from the Ministry of Education, Culture, Sports, Science, and Technology, by the Core Research for Evolutional Science and Technology program of the Japan Science and Technology Agency to K.O., and by the Excellence Initiative of the German Federal and State Governments (EXC 294), SFB 592, and the Landestiftung to K.P.

Received May 21, 2009; revised September 24, 2009; accepted October 15, 2009; published October 30, 2009.

REFERENCES

Abas, L., Benjamins, R., Malenica, N., Paciorek, T., Wisniewska, J., Moulinier-Anzola, J.C., Sieberer, T., Friml, J., and Luschnig, C. (2006). Intracellular trafficking and proteolysis of the *Arabidopsis* auxin-efflux facilitator PIN2 are involved in root gravitropism. Nat. Cell Biol. **8:** 249–256.

Aida, M., Beis, D., Heidstra, R., Willemsen, V., Blilou, I., Galinha, C., Nussaume, L., Noh, Y.-S., Amasino, R., and Scheres, B. (2004). The *PLETHORA* genes mediate patterning of the *Arabidopsis* root stem cell niche. Cell **119:** 109–120.

Baima, S., Nobili, F., Sessa, G., Lucchetti, S., Ruberti, I., and Morelli, G. (1995). The expression of the *Athb-8* homeobox gene is restricted to provascular cells in *Arabidopsis thaliana.* Development **121:** 4171–4182.

Bayer, E.M., Smith, R.S., Mandel, T., Nakayama, N., Sauer, M., Prusinkiewicz, P., and Kuhlemeier, C. (2009). Integration of transport-based models for phyllotaxis and midvein formation. Genes Dev. **23:** 373–384.

Bennett, T., Sieberer, T., Willett, B., Booker, J., Luschnig, C., and Leyser, O. (2006). The *Arabidopsis MAX* pathway controls shoot branching by regulating auxin transport. Curr. Biol. **16:** 553–563.

Benková, E., Michniewicz, M., Sauer, M., Teichmann, T., Seifertová, E., Jürgens, G., and Friml, J. (2003). Local, efflux-dependent auxin gradients as a common module for plant organ formation. Cell **115:** 591–602.

Blilou, I., Xu, J., Wildwater, M., Willemsen, V., Paponov, I., Friml, J., Heidstra, R., Aida, M., Palme, K., and Scheres, B. (2005). The PIN auxin efflux facilitator network controls growth and patterning in *Arabidopsis* roots. Nature **433:** 39–44.

Bougourd, S., Marrison, J., and Haseloff, J. (2000). An aniline blue staining procedure for confocal microscopy and 3D imaging of normal and perturbed cellular phenotypes in mature *Arabidopsis* embryos. Plant J. **24:** 543–550.

Boutté, Y., Crosnier, M.-T., Carraro, N., Traas, J., and Satiat-Jeunemaitre, B. (2005). The plasma membrane recycling pathway and cell polarity in plants: Studies on PIN proteins. J. Cell Sci. **119:** 1255–1265.

Colón-Carmona, A., You, R., Hamimovitch-Gal, T., and Doerner, P. (1999). Spatio-temporal analysis of mitotic activity with a labile cyclin-GUS fusion protein. Plant J. **20:** 503–508.

Ditengou, F.A., Teale, W.D., Kochersperger, P., Flittner, K.A., Kneuper, I., van der Graaff, E., Nziengui, H., Pinosa, F., Li, X., Nitschke, R., Laux, T., and Palme, K. (2008). Mechanical induction of lateral root initiation in *Arabidopsis thaliana.* Proc. Natl. Acad. Sci. USA **105:** 18818–18823.

Dhonukshe, P., et al. (2008). Generation of cell polarity in plants links endocytosis, auxin distribution and cell fate decisions. Nature **456:** 962–966.

Dutta, R., and Inouye, M. (2000). GHKL, an emergent ATPase/kinase superfamily. Trends Biochem. Sci. **25:** 24–28.

Engert, J.C., et al. (2000). ARSACS, a spastic ataxia common in northeastern Québec, is caused by mutations in a new gene encoding an 11.5-kb ORF. Nat. Genet. **24:** 120–125.

Friml, J., Benková, E., Blilou, I., Wisniewska, J., Hamann, T., Ljung, K., Woody, S., Sandberg, G., Scheres, B., Jürgens, G., and Palme, K. (2002a). AtPIN4 mediates sink-driven auxin gradients and root patterning in *Arabidopsis.* Cell **108:** 661–673.

Friml, J., Wisniewska, J., Benková, E., Mendgen, K., and Palme, K. (2002b). Lateral relocation of auxin efflux regulator PIN3 mediates tropism in *Arabidopsis.* Nature **415:** 806–809.

Friml, J., Vieten, A., Sauer, M., Weijers, D., Schwarz, H., Hamann, T., Offringa, R., and Jürgens, G. (2003). Efflux-dependent auxin gradients establish the apical-basal axis of *Arabidopsis.* Nature **426:** 147–153.

Friml, J., et al. (2004). A PINOID-dependent binary switch in apical-basal PIN polar targeting directs auxin efflux. Science **306:** 862–865.

Furutani, M., Vernoux, T., Traas, J., Kato, T., Tasaka, M., and Aida, M. (2004). *PIN-FORMED1* and *PINOID* regulate boundary formation and cotyledon development in *Arabidopsis* embryogenesis. Development **131:** 5021–5030.

Galinha, C., Hofhuis, H., Luijten, M., Willemsen, V., Blilou, I., Heidstra, R., and Scheres, B. (2007). PLETHORA proteins as dose-dependent master regulators of *Arabidopsis* root development. Nature **449:** 1053–1057.

Gälweiler, L., Guan, C., Müller, A., Wisman, E., Mendgen, K., Yephremov, A., and Palme, K. (1998). Regulation of polar auxin transport by AtPIN1 in *Arabidopsis* vascular tissue. Science **282:** 2226–2230.

Geldner, N., Anders, N., Wolters, H., Keicher, J., Kornberger, W., Muller, P., Delbarre, A., Ueda, T., Nakano, A., and Jürgens, G. (2003). The *Arabidopsis* GNOM ARF-GEF mediates endosomal recycling, auxin transport, and auxin-dependent plant growth. Cell **112:** 219–230.

Geldner, N., Friml, J., Stierhof, Y.-D., Jürgens, G., and Palme, K. (2001). Auxin transport inhibitors block PIN1 cycling and vesicle trafficking. Nature **413:** 425–428.

Geldner, N., Richter, S., Vieten, A., Marquardt, S., Torres-Ruiz, R.A., Mayer, U., and Jürgens, G. (2004). Partial loss-of-function alleles reveal a role for *GNOM* in auxin transport-related, post-embryonic development of *Arabidopsis.* Development **131:** 389–400.

Hardtke, C.S., and Berleth, T. (1998). The *Arabidopsis* gene *MONOPTEROS* encodes a transcription factor mediating embryo axis formation and vascular development. EMBO J. **17:** 1405–1411.

Hardtke, C.S., Ckurshumova, W., Vidaurre, D.P., Singh, S.A., Stamatiou, G., Tiwari, S.B., Hagen, G., Tom, J., Guilfoyle, T.J., and Berleth, T. (2004). Overlapping and non-redundant functions of the Arabidopsis auxin response factors *MONOPTEROS* and *NONPHOTOTROPIC HYPOCOTYL 4.* Development **131:** 1089–1100.

Heisler, M.G., Ohno, C., Das, P., Sieber, P., Reddy, G.V., Long, J.A., and Meyerowitz, E.M. (2005). Patterns of auxin transport and gene expression during primordium development revealed by live imaging of the *Arabidopsis* inflorescence meristem. Curr. Biol. **15:** 1899–1911.

Helariutta, Y., Fukaki, H., Wysocka-Diller, J., Nakajima, K., Jung, J., Sena, G., Hauser, M.-T., and Benfey, P.N. (2000). The *SHORT-ROOT* gene controls radial patterning of the *Arabidopsis* root through radial signaling. Cell **101:** 555–567.

Jaillais, Y., Santambrogio, M., Rozier, F., Fobis-Loisy, I., Miege, C., and Gaude, T. (2007). The retromer protein VPS29 links cell polarity and organ initiation in plants. Cell **130:** 1057–1070.

Kawakami, S., and Watanabe, Y. (1997). Use of green fluorescent protein as a molecular tag of protein movement *in vivo.* Plant Biotechnol. **14:** 127–130.

Kleine-Vehn, J., Dhonukshe, P., Sauer, M., Brewer, P.B., Wisniewska, J., Paciorek, T., Benková, E., and Friml, L. (2008a). ARF GEF-dependent transcytosis and polar delivery of PIN auxin carriers in *Arabidopsis.* Curr. Biol. **18:** 526–531.

Kleine-Vehn, J., Leitner, J., Zwiewka, M., Sauer, M., Abas, L., Luschnig, C., and Friml, J. (2008b). Differential degradation of PIN2 auxin efflux carrier by retromer-dependent vacuolar targeting. Proc. Natl. Acad. Sci. USA **105:** 17812–17817.

Kornet, N., and Scheres, B. (2009). Members of the GCN5 histone acetyltransferase complex regulate PLETHORA-mediated root stem cell niche maintenance and transit amplifying cell proliferation in *Arabidopsis.* Plant Cell **21:** 1070–1079.

Laplaze, L., Parizot, B., Baker, A., Ricaud, L., Martiniere, A., Auguy, F., Franche, C., Nussaume, L., Bogusz, D., and Haseloff, J. (2005). GAL4-GFP enhancer trap lines for genetic manipulation of lateral root development in *Arabidopsis thaliana.* J. Exp. Bot. **56:** 2433–2442.

Laskowski, M., Grieneisen, V.A., Hofhuis, H., ten Hove, C.A., Hogeweg, P., Marée, A.F.M., and Scheres, B. (2008). Root system architecture from coupling cell shape to auxin transport. PLoS Biol. **6:** 2721–2735.

Laxmi, A., Pan, J., Morsy, M., and Chen, R. (2008). Light plays an essential role in intracellular distribution of auxin efflux carrier PIN2 in *Arabidopsis thaliana.* PLoS One **3:** e1510.

Liu, C., Xu, Z., and Chua, N.H. (1993). Auxin polar transport is essential for the establishment of bilateral symmetry during early plant embryogenesis. Plant Cell **5:** 621–630.

Mattsson, J., Ckurshumova, W., and Berleth, T. (2003). Auxin signaling in *Arabidopsis* leaf vascular development. Plant Physiol. **131:** 1327–1339.

Mattsson, J., Sung, Z.R., and Berleth, T. (1999). Responses of plant vascular systems to auxin transport inhibition. Development **126:** 2979–2991.

Mayer, U., Büttner, G., and Jürgens, G. (1993). Apical-basal pattern formation in the *Arabidopsis* embryo: studies on the role of the *gnom* gene. Development **117:** 149–162.

Michniewicz, M., et al. (2007). Antagonistic regulation of PIN phosphorylation by PP2A and PINOID directs auxin flux. Cell **130:** 1044–1056.

Nakagawa, T., et al. (2007). Improved Gateway binary vectors: High-performance vectors for creation of fusion constructs in transgenic analysis of plants. Biosci. Biotechnol. Biochem. **71:** 2095–2100.

Ottenschläger, I., Wolff, P., Wolverton, C., Bhalerao, R.P., Sandberg, G., Ishikawa, H., Evans, M., and Palme, K. (2003). Gravity-regulated differential auxin transport from columella to lateral root cap cells. Proc. Natl. Acad. Sci. USA **100:** 2987–2991.

Paciorek, T., Zazímalová, E., Ruthardt, N., Petrásek, J., Stierhof, Y.-D., Kleine-Vehn, J., Morris, D.A., Emans, N., Jürgens, G., Geldner, N., and Friml, J. (2005). Auxin inhibits endocytosis and promotes its own efflux from cells. Nature **435:** 1251–1256.

Paponov, I.A., Teale, W.D., Trebar, M., Blilou, I., and Palme, K. (2005). The PIN auxin efflux facilitators: evolutionary and functional perspectives. Trends Plant Sci. **10:** 170–177.

Petrásek, J., et al. (2006). PIN proteins perform a rate-limiting function in cellular auxin efflux. Science **312:** 914–918.

Pierik, R., Djakovic-Petrovic, T., Keuskamp, D.H., de Wit, M., and Voesenek, L.A.C.J. (2009). Auxin and ethylene regulate elongation responses to neighbor proximity signals independent of gibberellin and DELLA proteins in *Arabidopsis.* Plant Physiol. **149:** 1701–1712.

Pyo, H., Demura, T., and Fukuda, H. (2004). Spatial and temporal tracing of vessel differentiation in young *Arabidopsis* seedlings by the expression of an immature tracheary element-specific promoter. Plant Cell Physiol. **45:** 1529–1536.

Reinhardt, D., Mandel, T., and Kuhlemeier, C. (2000). Auxin regulates the initiation and radial position of plant lateral organs. Plant Cell **12:** 507–518.

Reinhardt, D., Pesce, E.-R., Stieger, P., Mandel, T., Baltensperger, K., Bennett, M., Traas, J., Friml, J., and Kuhlemeier, C. (2003). Regulation of phyllotaxis by polar auxin transport. Nature **426:** 255–260.

Sabatini, S., Beis, D., Wolkenfelt, H., Murfett, J., Guilfoyle, T., Malamy, J., Benfey, P., Leyser, O., Bechtold, N., Weisbeek, P., and Scheres, B. (1999). An auxin-dependent distal organizer of pattern and polarity in the *Arabidopsis* root. Cell **99:** 463–472.

Sabatini, S., Heidstra, R., Wildwater, M., and Scheres, B. (2003). SCARECROW is involved in positioning the stem cell niche in the *Arabidopsis* root meristem. Genes Dev. **17:** 354–358.

Sachs, T. (1991). Cell polarity and tissue patterning in plants. Dev. Suppl. **1:** 83–93.

Sarkar, A.K., Luijten, M., Miyashima, S., Lenhard, M., Hashimoto, T., Nakajima, K., Scheres, B., Heidstra, R., and Laux, T. (2007). Conserved factors regulates signaling in *Arabidopsis thaliana* shoot and root stem cell organizers. Nature **446:** 811–814.

Sauer, M., Balla, J., Luschnig, C., Wisniewska, J., Reinöhl, V., Friml, J., and Benková, E. (2006). Canalization of auxin flow by Aux/IAA-ARF-dependent feedback regulation of PIN polarity. Genes Dev. **20:** 2902–2911.

Scarpella, E., Marcos, D., Friml, J., and Berleth, T. (2006). Control of leaf vascular patterning by polar auxin transport. Genes Dev. **20:** 1015–1027.

Shirakawa, M., Ueda, H., Shimada, T., Nishiyama, C., and Hara-Nishimura, I. (2009). Vacuolar SNAREs function in the formation of the leaf vascular network by regulating auxin distribution. Plant Cell Physiol. **50:** 1319–1328.

Sieberer, Y., Seifert, G.J., Hauser, M.-T., Grisafi, P., Fink, G.R., and Luschnig, C. (2000). Post-transcriptional control of the *Arabidopsis* auxin efflux carrier EIR1 requires AXR1. Curr. Biol. **10:** 1595–1598.

Sieburth, L.E. (1999). Auxin is required for leaf vein pattern in *Arabidopsis.* Plant Physiol. **121:** 1179–1190.

Spitzer, C., Reyes, F.C., Buono, R., Sliwinski, M.K., Haas, T.J., and Otegui, M.S. (2009). The ESCRT-related CHMP1A and B proteins mediate multivesicular body sorting of auxin carriers in *Arabidopsis* and are required for plant development. Plant Cell **21:** 749–766.

Steinmann, T., Geldner, N., Grebe, M., Mangold, S., Jackson, C.L., Paris, S., Gälweiler, L., Palme, K., and Jürgens, G. (1999). Coordinated polar localization of auxin efflux carrier PIN1 by GNOM ARF GEF. Science **286:** 316–318.

Tsugeki, R., Kochieva, E.Z., and Fedoroff, N.V. (1996). A transposon insertion in the *Arabidopsis SSR16* gene causes an embryo-defective lethal mutation. Plant J. **10:** 479–489.

Ulmasov, T., Murfett, J., Hagen, G., and Guilfoyle, T.J. (1997). Aux/IAA proteins repress expression of reporter genes containing natural and highly active synthetic auxin response elements. Plant Cell **9:** 1963–1971.

van den Berg, C., Willemsen, V., Hendriks, G., Weisbeek, P., and Scheres, B. (1997). Short-range control of cell differentiation in the *Arabidopsis* root meristem. Nature **390:** 287–289.

Vieten, A., Vanneste, S., Wisniewska, J., Benková, E., Benjamins, R., Beeckman, T., Luschnig, C., and Friml, J. (2005). Functional redundancy of PIN proteins is accompanied by auxin-dependent cross-regulation of PIN expression. Development **132:** 4521–4531.

Wenzel, C.L., Schuetz, M., Yu, Q., and Mattsson, J. (2007). Dynamics of *MONOPTEROS* and PIN-FORMED1 expression during leaf vein pattern formation in *Arabidopsis thaliana.* Plant J. **49:** 387–398.

Willemsen, V., Friml, J., Grebe, M., van den Toorn, A., Palme, K., and Scheres, B. (2003). Cell polarity and PIN protein positioning in *Arabidopsis* require *STEROL METHYLTRANSFERASE1* function. Plant Cell **15:** 612–625.

Wisniewska, J., Xu, J., Seifertová, D., Brewer, P.B., Ruzicka, K., Blilou, I., Rouquié, D., Benková, E., Scheres, B., and Friml, J. (2006). Polar PIN localization directs auxin flow in plants. Science **312:** 883.

Wysocka-Diller, J.W., Helariutta, Y., Fukaki, H., Malamy, J.E., and Benfey, P.N. (2000). Molecular analysis of SCARECROW function reveals a radial patterning mechanism common to root and shoot. Development **127:** 595–603.

Xu, J., Hofhuis, H., Heidstra, R., Sauer, M., Friml, J., and Scheres, B. (2006). A molecular framework for plant regeneration. Science **311:** 385–388.

Yadav, R.K., Girke, T., Pasala, S., Xie, M., and Reddy, G.V. (2009). Gene expression map of the *Arabidopsis* shoot apical meristem stem cell niche. Proc. Natl. Acad. Sci. USA **106:** 4941–4946.